Rock Mechanics and Rock Engineering (2020) 53:31–57
https://doi.org/10.1007/s00603-019-01866-w

ORIGINAL PAPER

Effect of Cyclic Loading on the Shear Behaviours of Both Unfilled and Infilled Rough Rock Joints Under Constant Normal Stiffness Conditions

Guansheng Han[1,2] · Hongwen Jing[1] · Yujing Jiang[2] · Richeng Liu[1,2] · Jiangyu Wu[1]

Received: 19 December 2018 / Accepted: 20 May 2019 / Published online: 21 June 2019

Abstract

The present study experimentally investigated variations in the mechanical behaviours of natural rough rock joints during shearing under cyclic loading and constant normal stiffness conditions, using a servo-controlled shear testing apparatus. The influences of initial normal stress (σ_{n0}), normal stiffness (k_n) and shear velocity (v) on the shear behaviours are estimated and analysed. The results show that the shear stress (τ), normal stress (σ_n) and normal displacement (δ_v) for both unfilled and infilled rock joints decrease with the increase in the number of cycles (N), especially in the N range of 1–2. This is because some asperities on the joint surface are sheared during the first shear process, and the subsequent shear tests for $N > 2$ were subjected to the frictional process. The σ_{n0} and k_n both contribute significantly to the variations in the shear behaviour of rock joints. For unfilled rock joints, increasing σ_{n0} from 2 to 4 MPa increases the shear stress and normal stress by 128.5% and 106.5%, respectively, when shear displacement (δ_h) = 2 mm and $N = 1$. Increasing k_n from 3 to 5 GPa/m enhances the shear stress and normal stress by 19.4% and 10.4%, respectively, when $\delta_h = 2$ mm and $N = 1$. For infilled rock joints, the shear stress and normal stress increase with increasing σ_{n0} when $N < 5$, and decrease first and then increase with increasing k_n. The shear stress, normal stress and normal displacement for infilled rock joints increase with increasing v, especially in the v range of 1–2 mm/min. Finally, six empirical models are proposed to evaluate the shear stress, normal stress and normal displacement of the unfilled and infilled rock joints under cyclic loading and CNS conditions. These models take into account parameters such as σ_{n0}, k_n, v, δ_h and N, and the experimental results agree well with the fitting results with the correlation coefficient $R^2 > 0.78$. Using the proposed models, the fillings decrease the τ and σ_n by approximately 24.96–65.52% and 9.38–57.95%, respectively, while increasing the normal displacement (δ_v) by 0.5 mm on average during the entire shear process.

Keywords Rock joint · Surface roughness · Shear · Cyclic loading · Constant normal stiffness

1 Introduction

The shear stress and deformation characteristics of rock joints under cyclic loading are the mechanistic underpinnings for analysing the stability of geotechnical engineering under seismic loading (Jafari et al. 2004; Mirzaghorbanali et al. 2014). Cyclic shear loading causes wear and passivation on the surface of rock joints, thereby deteriorating the shear-related mechanical parameters of rock joints such as peak shear stress and residual shear stress. The rock mass dislocates and slips along the joint plane, resulting in the deformation and failure of geological engineering structures (Wu et al. 2018a). Therefore, it is of great significance in the understanding of the variation in the shear behaviour of natural rock joints under cyclic loading and constant normal stiffness (CNS) conditions.

The mechanical properties of rock joints can directly affect the stability of rock masses, which is a consistent research topic of interest in the field of geotechnical engineering (Bahaaddini 2017). A large number of laboratory tests have been devoted to the strength characteristics of rock joints such as uniaxial compressive strength (Liu et al. 2017a, b, 2018), biaxial compressive strength (Han et al.

✉ Yujing Jiang
jiang@nagasaki-u.ac.jp

[1] State Key Laboratory for Geomechanics and Deep Underground Engineering, China University of Mining and Technology, Xuzhou 221116, Jiangsu, China

[2] Graduate School of Engineering, Nagasaki University, Nagasaki 852-8521, Japan

2018a, b), triaxial compressive strength (Han et al. 2018a, b), dynamic strength (Li et al. 2001; Fathi et al. 2016), fatigue behaviour (Wu et al. 2014; Luo et al. 2016), monotonic shear strength under constant normal load (CNL) (Barton 1973), monotonic shear strength under CNS (Indraratna et al. 2015) and tensile strength (Shang et al. 2018). Other studies have investigated the shear behaviours of rock joints under cyclic shear loading. Under a CNL boundary condition, Jaeger (1971) and Plesha (1987) conducted cyclic shear tests on fresh rock joints. Their results showed that the specimens have a high shear stress in the first cycle of the shear test, and there are no obvious peak and residual shear stresses until the number of cycles (*N*) is larger than 15. Later, a two-dimensional constitutive model was proposed by Jing et al. (1993) to estimate the shear behaviour of rock joints under monotonic and cyclic loadings. Lee et al. (2001) conducted a large number of experiments on granite and marble specimens under cyclic loading, and an elastoplastic constitutive model was proposed based on their experimental results. Other similar studies have been reported by Hutson and Dowding (1990), Kana et al. (1996), Fox et al. (1998) and Homand et al. (2001). However, in the case of deep underground scenarios, the CNS boundary condition is more applicable than the CNL condition because the normal stress that is applied perpendicular to the direction of shear is not a constant for many field situations (Heuze 1979; Indraratna et al. 1999; Jiang et al. 2004). A few studies have investigated the effect of the CNS boundary condition on the shear behaviour of rock joints under cyclic loading. Belem et al. (2007, 2009) scanned and quantified the surface damage for different shearing cycles under CNS conditions, and two generalized joint surface asperity degradation models were proposed. Mirzaghorbanali et al. (2014) studied the variations in the shear behaviour of infilled rock joints under cyclic loading, and a mathematical model considering initial asperity angle, initial normal stress and ratio of infill thickness to asperity height was proposed. Most of the current studies are devoted to the shear behaviour of rock joints with regular surfaces, such as a saw-toothed joint (Oh et al. 2017) and/or under CNL conditions. However, natural rock joints are mostly rough/irregular, and a naturally rough rock joint under a CNS condition inhibits the shear-induced dilation (Li et al. 2018). To the best of our knowledge, the shear behaviour of natural rough rock joints under cyclic loading and CNS conditions has not been studied, if any.

The present study investigates the shear behaviour of natural rock joints under cyclic loading and CNS conditions, using a servo-controlled shear testing apparatus. Both unfilled and infilled rock joints are tested by taking into account the influences of initial normal stress (σ_{n0}), normal stiffness (k_n) and shear velocity (v). The predicted shear stress (τ), normal stress (σ_n) and normal displacement (δ_v) using the proposed regression functions are compared with the experimental results of both unfilled and infilled rock joints under CNS conditions.

2 Experiments

2.1 Testing System

The shear tests under cyclic loading and CNS conditions were carried out using the MIS-233-1-55-03 servo-controlled direct shear apparatus, which was designed and manufactured by Jiang et al. (2004) at Nagasaki University. Figure 1 shows a schematic view of the shear apparatus in detail. The apparatus can automatically reproduce various boundary conditions with a good accuracy, i.e., CNL, CNS and constant normal displacement boundary conditions, for shearing rock joints. Five linear variable differential

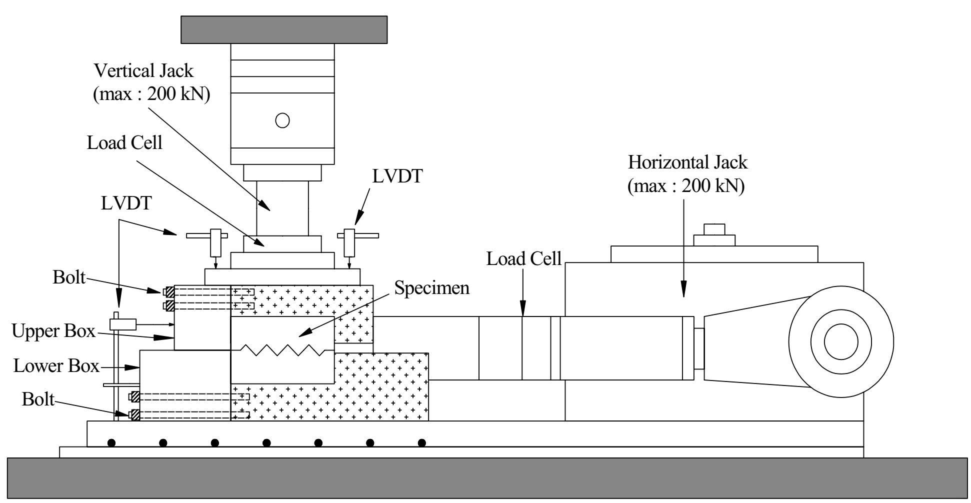

Fig. 1 Digitally controlled shear testing apparatus

transformers (LVDTs) with an accuracy of 0.001 mm are used. One LVDT is installed on the lower shear box to measure the shear displacement, and another four LVDTs are placed on the four corners of the upper shear box to measure the normal displacement. The data acquisition and instrumentation systems were designed using the LabVIEW programming language, which is controlled by a personal computer. The loading capacity is 200 kN in both the normal and shear directions, and the maximum shear displacement is 20 mm.

2.2 Surface Morphology and Specimen Preparation

The joint has a natural surface copied from the field of an underground power station in Japan, as shown in Fig. 2a. A 3D laser scanning profilometer system was utilized to measure the surface morphology, which has an accuracy of ± 20 μm in both the *x*- and *y*-directions and ± 10 μm in the height direction (Li et al. 2008). Figure 2b shows the 3D digitized surface of the joint surface. The variation in frequency versus asperity height is depicted in Fig. 2c, and the results show that the asperity height follows a Gaussian distribution (Adler et al. 2013) with a standard deviation of 1.56. The joint roughness coefficient (JRC) of the natural rough joint was calculated using Eqs. (1) and (2) proposed by Tse and Cruden (1979), which are widely accepted in rock mechanics and rock engineering (Liu et al. 2017a, b, c; Yin et al. 2017):

$$Z_2 = \left[\frac{1}{M} \sum \left(\frac{z_{i-1} - z_i}{x_{i-1} - x_i} \right)^2 \right]^{1/2}, \tag{1}$$

$$\mathrm{JRC} = 32.2 + 32.47 \log Z_2, \tag{2}$$

where x_i and z_i represent the coordinates of the joint surface profile and M is the number of sampling points along the length of a joint surface. The mean JRC value is 5.34 (Fig. 2d), which was evaluated by cutting the surface using 60 equidistant lines along the shear direction.

The specimen has a dimension of length × width × height = 200 × 100 × 100 mm, and the rock-like materials were made of mixtures of plaster, water and retardant with a weight ratio of 1:0.2:0.005 (Jiang et al. 2006). For the infilled rock joints, the filling thickness is 6 mm, and the filling materials were made of mixtures of plaster, sand and water in a weight ratio of 1:1:0.4. The density and uniaxial compressive strength are 1.546 g/cm^3 and 36 MPa for the filling materials and 2.066 g/cm^3 and 50 MPa for the rock-like materials, respectively. As shown in Fig. 2e, f, the height of the rock-like materials is 100 mm for unfilled specimens, and the heights of the rock-like materials and the filling materials are 94 mm and 6 mm, respectively, for infilled specimens. A total of 18 specimens were prepared, which were maintained at a constant temperature of 25 °C and placed in a humid box with a relative humidity of 95% for 28 days after the specimens were demoulded.

2.3 Experimental Procedure

The effects of σ_{n0}, k_n and v on the shear behaviour of natural rock joints under cyclic loading and CNS conditions are investigated. First, $k_n = 5$ GPa/m and $v = 1$ mm/min, and σ_{n0} is set to 2, 4, and 6 MPa for investigating the shear-induced variations in shear stress, normal stress and normal displacement for both unfilled and infilled specimens. Second, $\sigma_{n0} = 4$ MPa and $v = 1$ mm/min, and k_n is set to 3, 5, 7 GPa/m. Finally, $\sigma_{n0} = 4$ MPa and $k_n = 5$ GPa/m, and v is set to 1, 2, 3 mm/min (Wang et al. 2016; Wu et al. 2018b). The three steps guarantee that the influences of σ_{n0}, k_n and v can be individually estimated by fixing the other two parameters. Here, k_n was calculated based on the following equation (Johnston et al. 1987; Jiang et al. 2001):

$$k_n = \frac{E}{(1+\delta)r}, \tag{3}$$

where E and δ are the modulus and Poisson's ratio of rock mass, respectively, and r is the influenced radius.

Figure 3 shows the loading path in the cyclic loading test. Note that δ_h increases from 0 to 10 mm and then decreases from 10 to 0 mm, which is regarded as a shear cycle. The maximum shear displacement (10 mm) is 5% of the specimen length (200 mm), and the maximum cycle number is 6. The direction of shear tests is defined as positive when δ_h increases from 0 to 10 mm and negative when δ_h ranges from 10 to 0 mm.

3 Results and Analysis

3.1 Effect of σ_{n0} on the Shear Behaviour of Natural Rough Rock Joints

For unfilled rock joints, the shear stress increases with the increase in δ_h, as shown in Fig. 4a–c, g–i. Taking $\sigma_{n0} = 2$ MPa as an example, the average shear stress increases by a rate of 29.2% when δ_h increases at a 2-mm interval at $N = 3$. This is because the CNS condition increases the normal stress and inhibits joint dilation. The shear stress decreases slowly as N increases due to the asperity degradation of the joint surfaces. The shear stress greatly increases when σ_{n0} increases from 2 to 4 MPa; however, it is slightly affected when σ_{n0} increases from 4 to 6 MPa. This indicates that the

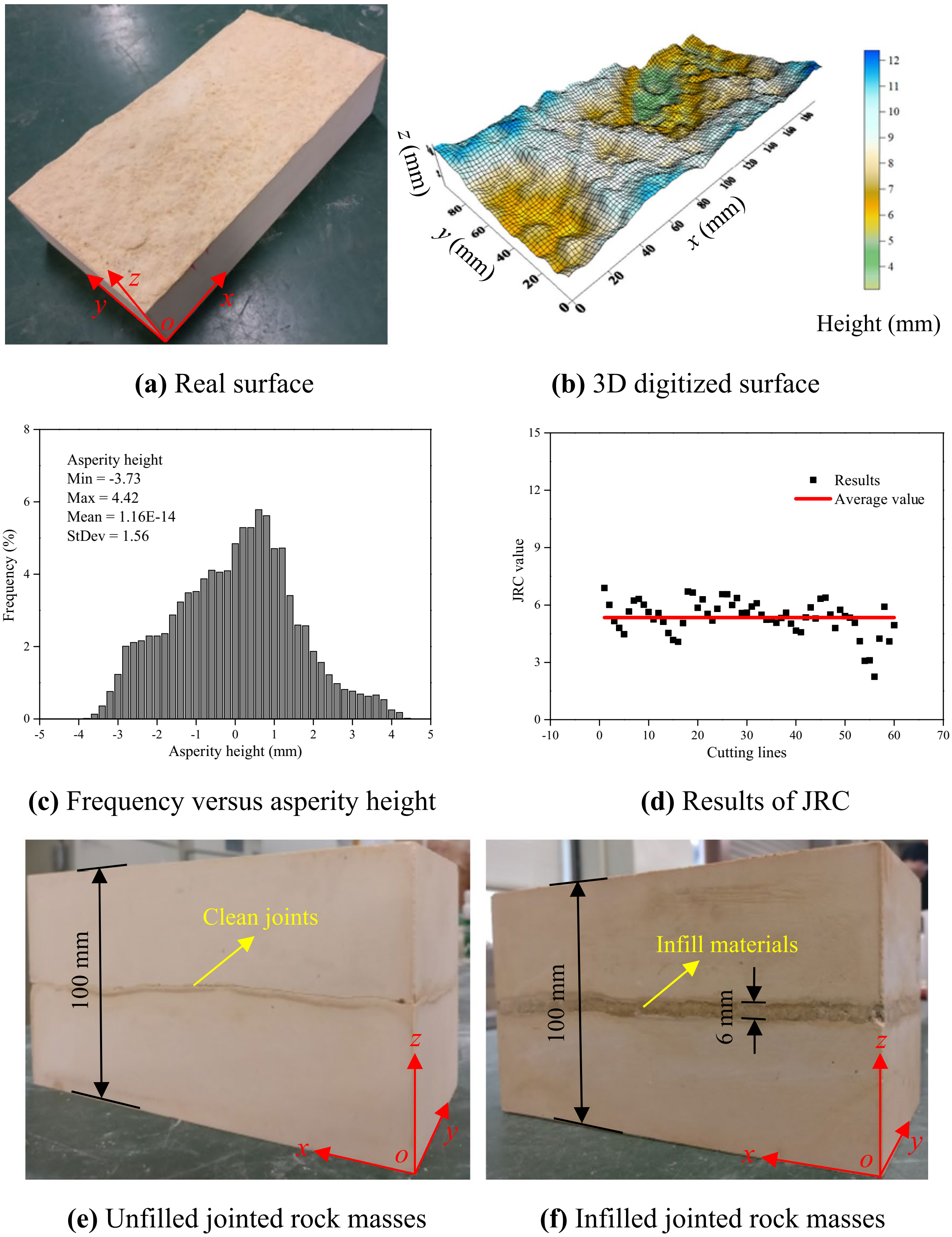

Fig. 2 Joint surfaces and specimens for tests

variation in shear stress is more sensitive to a smaller σ_{n0}. For infilled rock joints, the shear stress fluctuates slightly with the increase in δ_h, as shown in Fig. 4d–f, j–l, because the dilatation of rock joints during shearing is absorbed by the filling materials. The effect of σ_{n0} on the shear stress is obvious when $N < 4$ and is not remarkable when $N \geq 4$. The shear stress at the same shear displacement increases with the increase in σ_{n0} when the N is less than 4. Taking

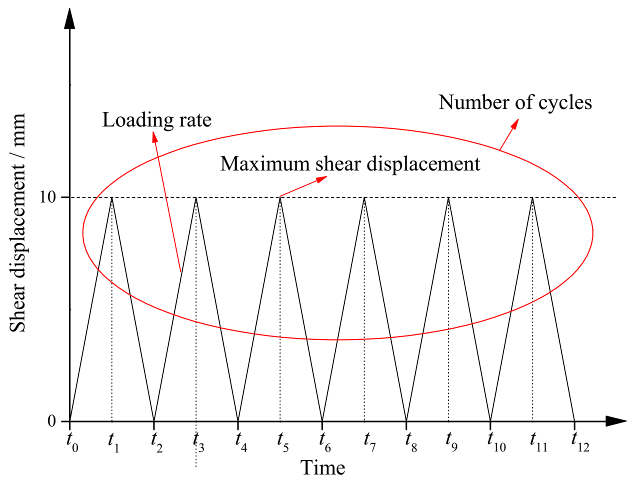

Fig. 3 The loading path in the cyclic loading test

$\delta_h = 2$ mm as an example, the shear stress increases from 1.77 to 2.74 MPa by a rate of 54.8% when σ_{n0} increases from 2 to 4 MPa for the first shear process. However, the effect of σ_{n0} on shear stress decreases and the decreasing rate decreases with increasing *N*. When $N = 6$ and $\delta_h = 2$ mm, the shear stress varies by a magnitude that is less than 0.13 MPa as σ_{n0} increases from 2 to 6 MPa.

The evolutions of normal stress of natural rock joints under different σ_{n0} are plotted in Fig. 5. The normal stress for unfilled rock joints increases with increasing δ_h and decreases as *N* increases, as shown in Fig. 5a–c, g–i. The δ_h has a slight effect on normal stress for infilled rock joints, and the normal stress decreases more significantly with increasing *N* from 1 to 6 for $\sigma_{n0} = 6$ MPa compared with that for $\sigma_{n0} = 2$ MPa, as shown in Fig. 5d–f, j–l. In the cyclic shear test, especially for the second and subsequent shear tests, the shear stress is mainly controlled by the frictional stress between the upper and lower surfaces of the joint due to the sheared-off bulges on the joint surface. It is widely accepted that there is a proportional relationship between the frictional stress and the normal stress (Belem et al. 2007, 2009; Mirzaghorbanali et al. 2014). The variations in normal stress with σ_{n0} follow similar trends to the shear stress.

The relationship between normal displacement and normal stress under CNS conditions can be expressed as follows:

$$\delta_v = \frac{\sigma_n - \sigma_{n0}}{k_n}. \tag{4}$$

Equation (4) indicates that the variation in δ_v is consistent with the variation in σ_n as long as σ_{n0} and k_n are fixed. Figure 6 shows the changes in the normal displacement of natural rock joints under different σ_{n0}. For unfilled rock joints, in each shear cycle, the δ_v increases as δ_h increases from 0 to 10 mm, which shows an obvious dilation, as shown in Fig. 6a–c, g–i. The δ_v decreases as δ_h decreases from 10 to 0 mm, which shows an obvious contraction. After six cycles of loading and unloading ($N = 6$), all the specimens show small amplitudes of contraction that are less than 0.2 mm. The normal displacement at the same shear displacement decreases with the increase in *N*. The δ_v shows a trend of rapid decline for $N = 1$–2 and a trend of slow decline for $N = 2$–6. The increase in σ_{n0} enlarges the downward trend of the two stages mentioned above. For infilled rock joints, the specimen shows a slight dilation in the positive direction of the first cycle and then exhibits different degrees of contraction in the subsequent cyclic shear tests, as shown in Fig. 6d–f, j–l. There is a downward trend for the normal displacement at the same shear displacement as *N* increases. The normal displacement increases more significantly for a larger σ_{n0}, which is consistent with Eq. (4). All the specimens show contractions after six cycles of loading and unloading, and the amount of contraction increases with the increase in σ_{n0}. For $\delta_h = 10$ mm, the specimens were contracted by 0.11, 0.61 and 1.13 mm, corresponding to $\sigma_{n0} = 2$, 4 and 6 MPa, respectively.

The failure modes of unfilled rock joints under different σ_{n0} values are shown in Fig. 7a–c. The asperities on the surface of the specimens are sheared off, and scratch marks obviously exist. By plotting the edges of the scratch marks, the damaged areas on the joint surface can be calculated using image processing. The damaged area increases from 85.7 to 130.7 cm^2 for σ_{n0} increasing from 2 to 4 MPa, by a rate of 52.5%. With continuously increasing σ_{n0} from 4 to 6 MPa, the damaged area increases from 130.7 to 139.8 cm^2 by a rate of 7% (Fig. 7d). This explains that the asperity damage, as well as the shear behaviour, is greatly influenced by $\sigma_{n0} = 2$–4 MPa, but is slightly affected by $\sigma_{n0} = 4$–6 MPa. However, for infilled rock joints, we found that even when the number of cycles is six, the shear-induced damage is concentrated on the filling materials and the surfaces/asperities of the joints are not scratched/crushed, which may be because of the large thickness (6.0 mm) of the fillings. The failure modes for the infilled joints after tests under different conditions such as different normal stiffness, different initial normal stresses and different shear velocities seem to be the same. Therefore, the area of the scratch marks of infilled rock joints is not presented and analyzed in the present study. In the future works, we will carry out cyclic shear tests under CNS conditions using rock joints infilled

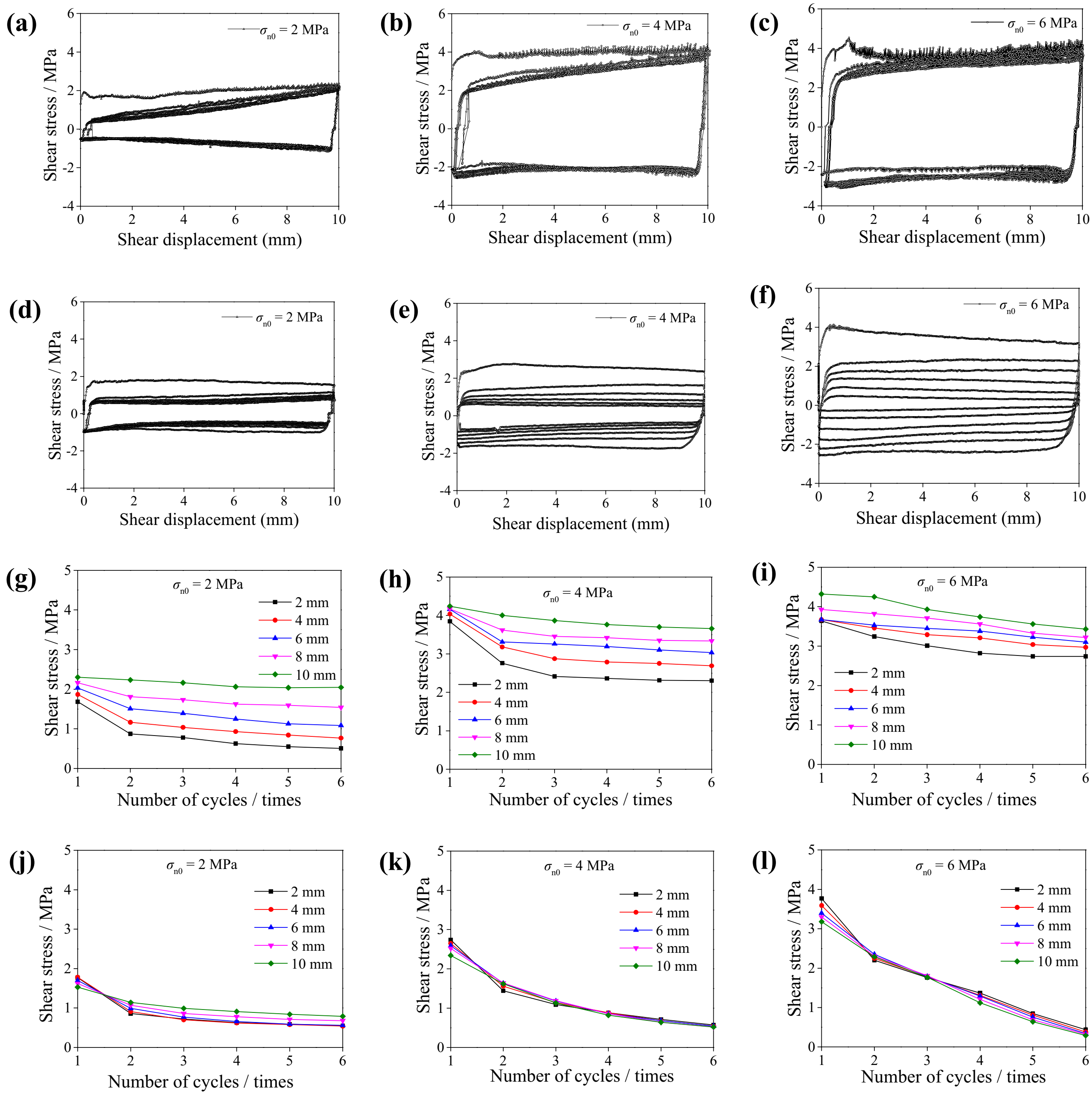

Fig. 4 **a–f** The variations in shear stress with varying shear displacements of unfilled and infilled rock joints, respectively, under different σ_{n0}; **g–l** shear stress versus number of cycles of unfilled and infilled rock joints, respectively, under different σ_{n0}

with materials having different thickness, and systematically investigate the influence of thickness of filling materials on the failure mode.

3.2 Effect of k_n on the Shear Behaviour of Natural Rough Rock Joints

Figure 8 depicts the evolution of the shear stress of natural rock joints under different k_n. For unfilled rock joints, as shown in Fig. 8a–c, g–i, the relationship between shear stress and N under different k_n is divided into a rapidly declining stage (N=1–2) and a slowly declining stage (N=2–6). The shear stress of the specimen increases with the increase in k_n because the larger k_n more significantly increases σ_n and requires a larger shear stress to shear the model. Taking N=1 as an example, the average shear stress, which is the average value of the shear stresses corresponding to δ_h=2, 4, 6, 8, 10 mm, for the first shear in the positive

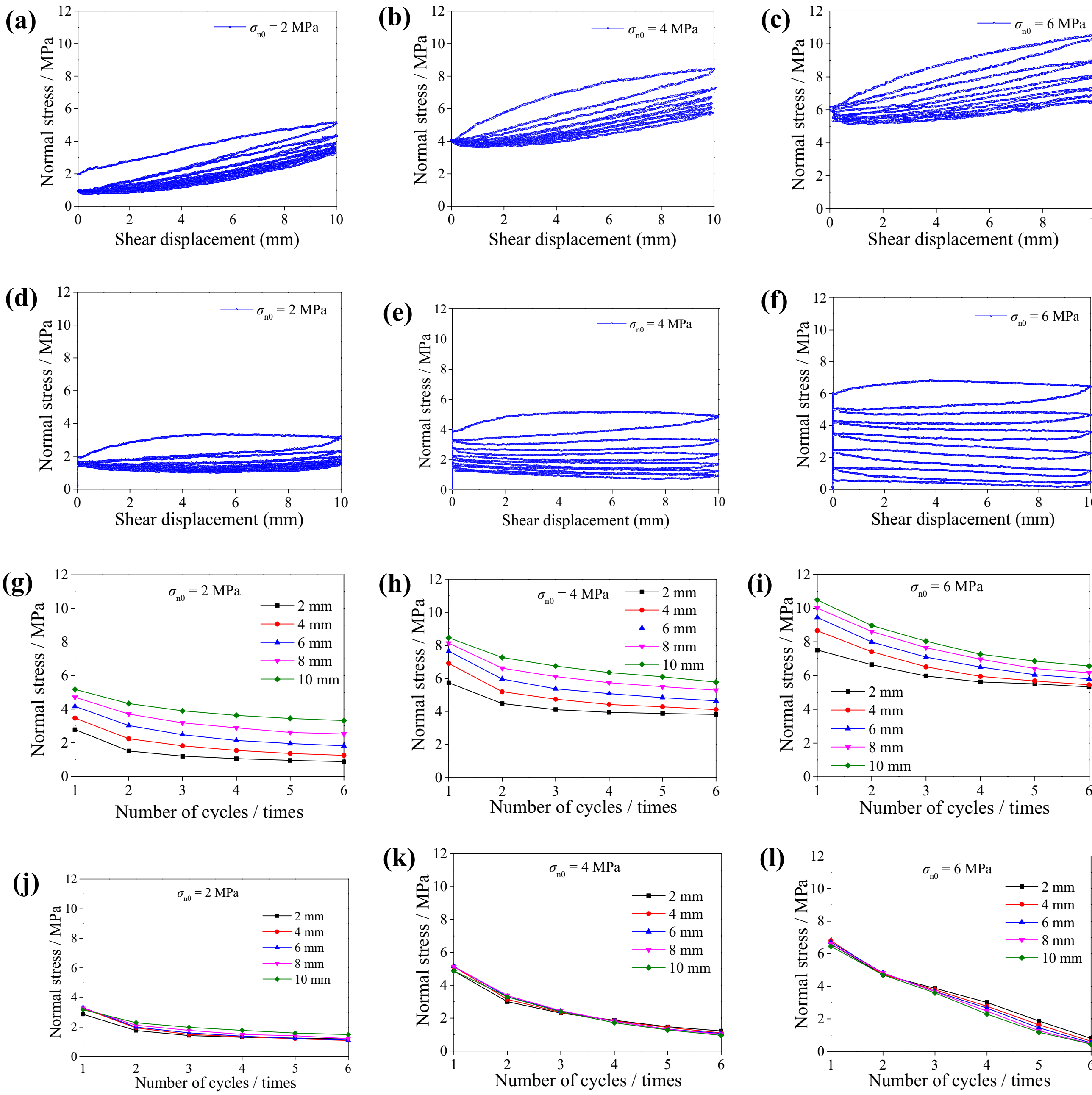

Fig. 5 **a–f** The variations in normal stress with varying shear displacements of unfilled and infilled rock joints, respectively, under different σ_{n0}; **g–l** normal stress versus number of cycles of unfilled and infilled rock joints, respectively, under different σ_{n0}

direction is 3.17, 4.09, and 4.12 MPa for $k_n = 3$, 5, and 7 GPa/m, respectively, which increases by 29.1% for k_n from 3 to 5 GPa/m and 0.8% for k_n from 5 to 7 GPa/m. For infilled rock joints, as shown in Fig. 8d–f, j–l, the average shear stress for the first shear in the positive direction is 2.57, 2.61, and 3.20 MPa for $k_n = 3$, 5, and 7 GPa/m, which shows an increase of 1.7% for $k_n = 3$–5 GPa/m, and 22.4% for $k_n = 5$–7 GPa/m. The results show that the shear stress of unfilled rock joints is more greatly influenced by k_n increasing from 3 to 5 GPa/m than that with $k_n = 5$–7 GPa/m. However, the shear stress of infilled rock joints is more greatly influenced by $k_n = 5$–7 GPa/m compared with that with $k_n = 3$–5 GPa/m.

The variations in the normal stress of natural rock joints under different k_n are presented in Fig. 9. For unfilled rock joints, the normal stress is very sensitive to k_n, as shown in Fig. 9a–c, g–i. For the first shear in the positive direction,

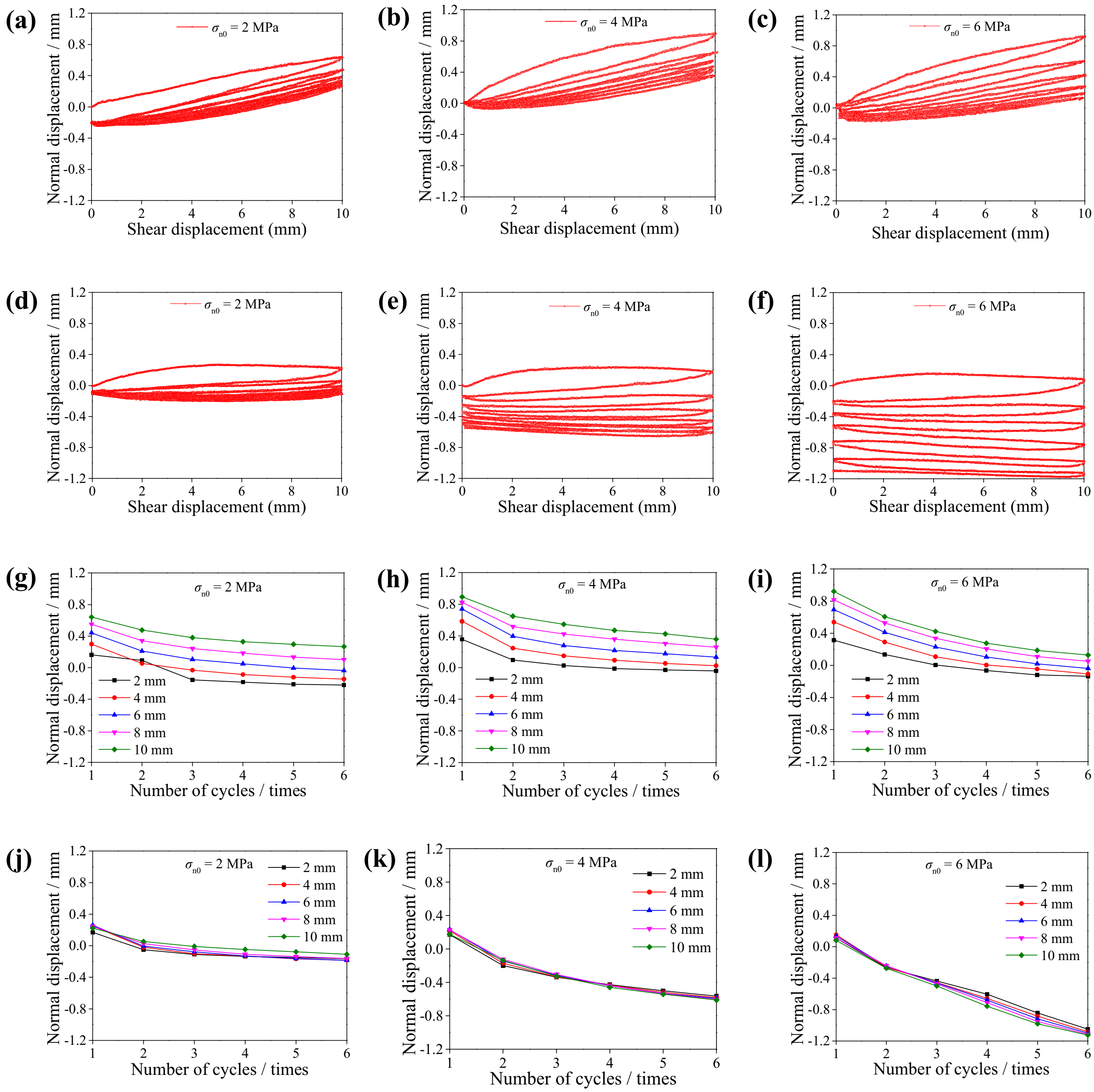

Fig. 6 **a–f** The variations in normal displacement with varying shear displacements of unfilled and infilled rock joints, respectively, under different σ_{n0}; **g–l** normal displacement versus number of cycles of unfilled and infilled rock joints, respectively, under different σ_{n0}

the maximum value of the normal stress is 7.31, 8.46 and 10.01 MPa for $k_n = 3$, 5 and 7 GPa/m, which increases by 82.8, 111.5 and 150.3% with respect to a constant σ_{n0} that is 4 MPa, as illustrated in Sect. 2.3. The normal stress increases with increasing δ_h, and increasing k_n increases the rate of the normal stress increment. To quantitatively analyse the effect of k_n on the increasing rate of the normal stress, K_v is defined as follows:

$$K_v = \left[\frac{1}{4} \sum_{i=2}^{8} \frac{\sigma_{n(i+2)} - \sigma_{n(i)}}{\sigma_{n(i)}} \right] \times 100\%, \quad (5)$$

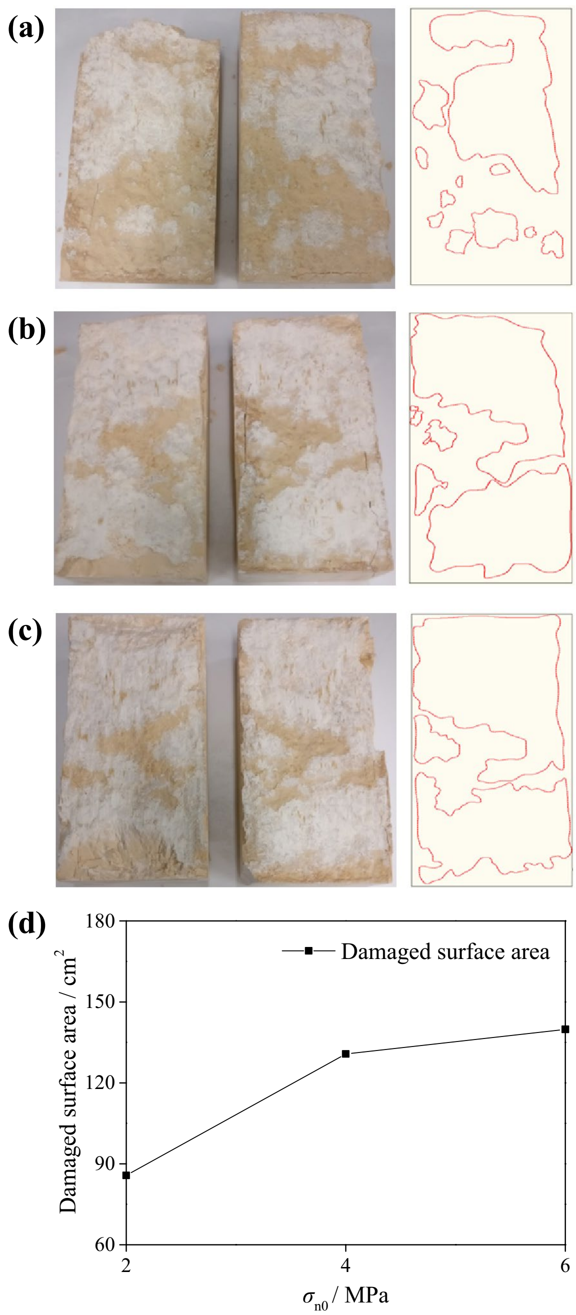

Fig. 7 Failure modes of unfilled rock joints under different σ_{n0}, **a** $\sigma_{n0}=2$ MPa, **b** $\sigma_{n0}=4$ MPa, **c** $\sigma_{n0}=6$ MPa, **d** damaged surface area vs. σ_{n0}

where $\sigma_{n(i)}$ is the normal stress corresponding to $\delta_h=i$, and $\sigma_{n(i+2)}$ is the normal stress corresponding to $\delta_h=i+2$, in which $i=2$, 4, 6, 8 mm. Taking $N=3$ as an example, K_v is 9.5, 13.2 and 15% when $k_n=3$, 5 and 7 GPa/m, respectively, showing a significant increase with the increase in k_n. In addition, the effect of k_n on the normal stress decreases with increasing N. When $N=1$ and $\delta_h=6$ mm, the normal stress varies in magnitudes of 6.50, 7.65, and 8.73 MPa, which are much larger than the magnitudes of 4.90, 4.61, and 4.74 MPa for $N=6$. However, the effect of k_n on the normal stress increases with the increase in N for the infilled rock joints (see Fig. 9j–l).

Figure 10 shows the relationships between normal displacement and shear displacement (or number of cycles) under different k_n for both unfilled and filled rock joints. When the rock joints are unfilled, the increase in k_n restrains the dilatation of joints. As a result, the δ_v decreases with increasing k_n when δ_h and N are fixed, and the δ_v is greatly affected as k_n increases from 3 to 5 GPa/m; however, it is slightly affected for $k_n=5$–7 GPa/m, as shown in Fig. 10a–c, g–i. In the first shear process of the positive direction, the maximum δ_v is 1.100, 0.893 and 0.868 mm for $k_n=3$, 5 and 7 GPa/m, which decreases by 18.8% when k_n increases from 3 to 5 GPa/m and decreases by 2.8% as k_n increases from 5 to 7 GPa/m, respectively. For infilled rock joints, a slight dilation occurs only for the first shear in the positive direction, and the specimens show obvious contractions after the first cyclic loading, as shown in Fig. 10d–f, j–l. The final δ_v is − 0.451, − 0.554, and − 0.209 mm as k_n is 3, 5 and 7 GPa/m when $N=6$, which indicates that the shear contraction of infilled rock joints under cyclic loading is slightly influenced by increasing k_n from 3 to 5 GPa/m but robustly affected when k_n increases from 5 to 7 GPa/m.

The failure modes of unfilled rock joints under different k_n are shown in Fig. 11. The damaged areas are 133.7, 130.7 and 131.6 cm^2 for $k_n=3$, 5 and 7 GPa/m, respectively, which are very close to the increment of k_n. This is because σ_{n0} is a constant that equals 4 MPa, and the normal stress increases with increasing k_n. All the specimens are subjected to a normal stress that is larger than 7 MPa, and the joint surface is dramatically damaged under such a high normal stress (see Fig. 9a–c).

3.3 Effect of *v* on the Shear Behaviour of Natural Rough Rock Joints

For unfilled rock joints, the variations in shear stress, normal stress and normal displacement with varying shear displacements are shown in Figs. 12a–c, 13a–c, and 14a–c, respectively, while those for infilled rock joints are shown in Figs. 12d–f, 13d–f, and 14d–f, respectively. The shear stress, normal stress and normal displacement for unfilled rock joints versus the number of cycles corresponding to shear displacements of 2, 4, 6, 8, 10 mm under different *v* are exhibited in Figs. 12g–i, 13g–i, and 14g–i, respectively, while those for infilled rock joints are shown in Figs. 12j–l,

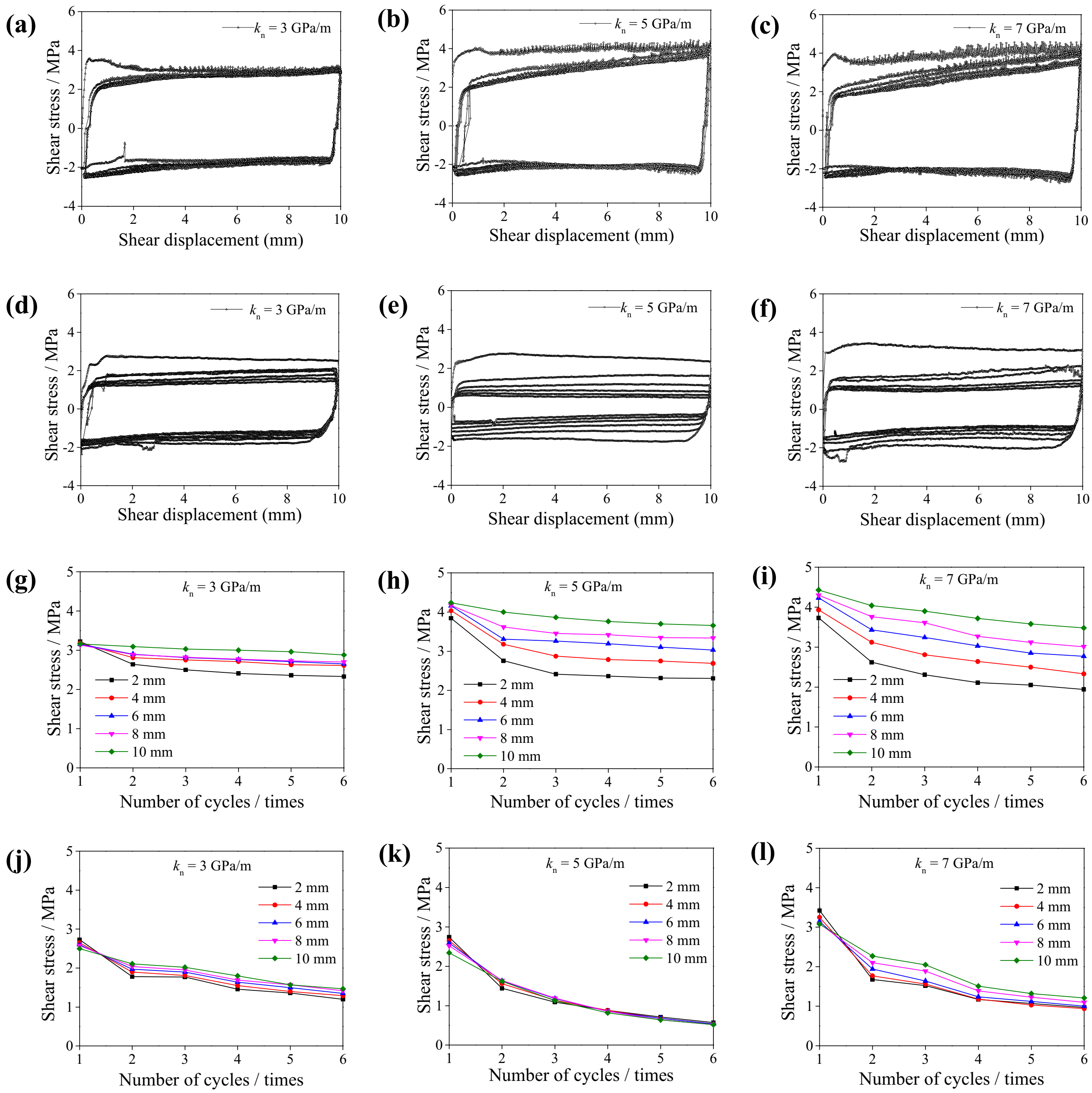

Fig. 8 **a–f** The variations in shear stress with varying shear displacements of unfilled and infilled rock joints, respectively, under different k_n; **g–i** and **j–l** shear stress versus number of cycles of unfilled and infilled rock joints, respectively, under different k_n

13j–l, and 14j–l, respectively. For unfilled rock joints, the shear stress decreases for v increasing from 1 to 2 mm/min and increases for v increasing from 2 to 3 mm/min. However, the normal stress and normal displacement increase for v increasing from 1 to 2 mm/min and decrease for v increasing from 2 to 3 mm/min. Figure 15 shows the failure modes of unfilled rock joints under different v, and the damaged area increases slightly with the increase in v. For infilled rock joints, the shear stress increases rapidly as v increases from 1 to 2 mm/min and increases slowly as v increases from 2 to 3 mm/min. Taking $N=3$ as an example, the shear stress in the positive direction at $\delta_h = 2$ mm increases from 1.09 to 1.36 MPa when v increases from 1 to 2 mm/min, which increases by 24.8%. When v increases from 2 to 3 mm/min,

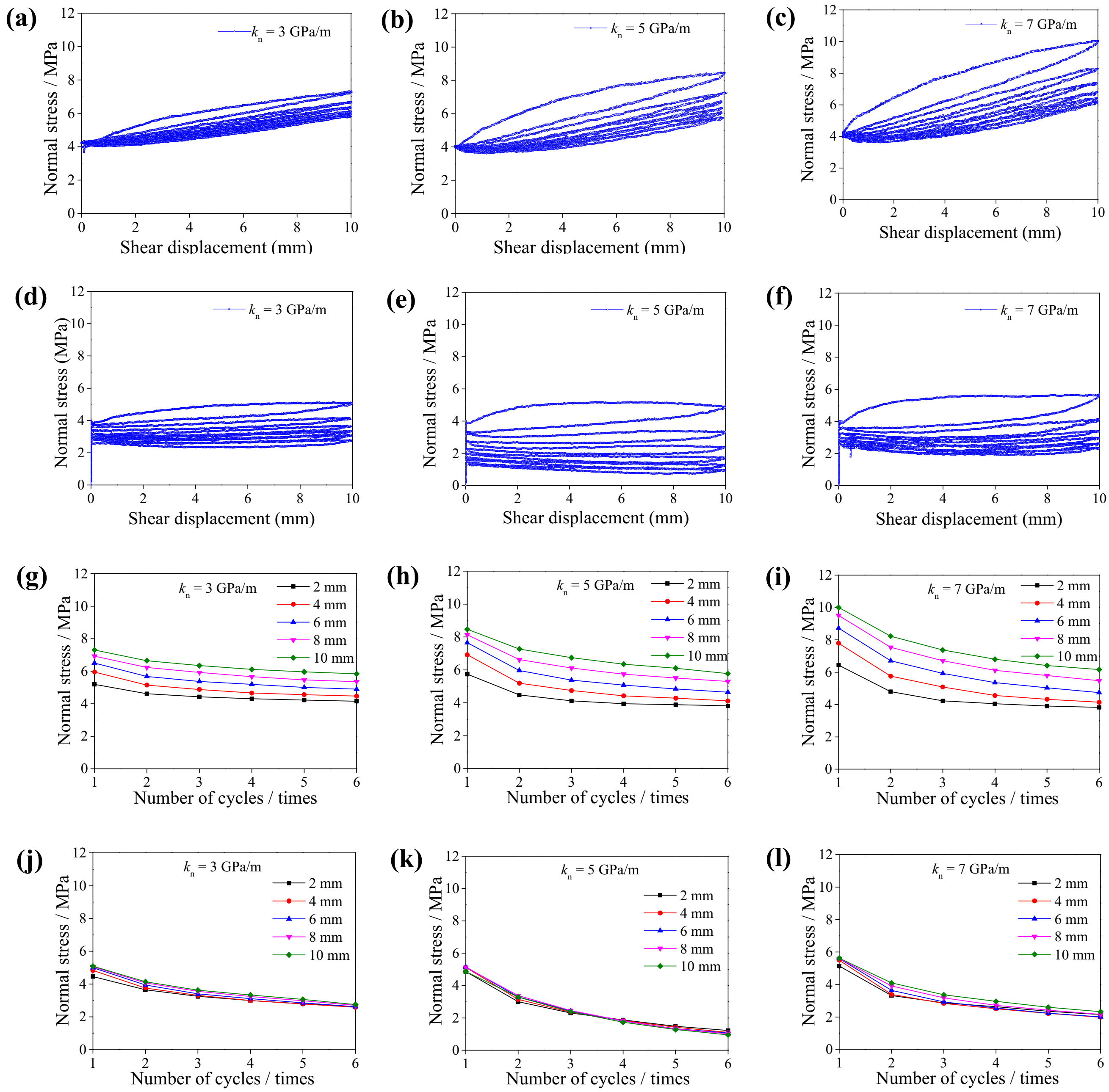

Fig. 9 **a–f** The variations in normal stress with varying shear displacements of unfilled and infilled rock joints, respectively, under different k_n; **g–l** normal stress versus number of cycles of unfilled and infilled rock joints, respectively, under different k_n

the shear stress increases from 1.36 to 1.37 MPa, at a rate of 0.7%. The variations in normal stress and the normal displacement of infilled rock joints versus N are consistent with the variation in the shear stress during shearing, as shown in Figs. 13j–l and 14j–l. The average normal stress, which is the average value of the normal stresses corresponding to $\delta_h = 2$, 4, 6, 8, 10 mm for the sixth shear cycle ($N = 6$) in the positive direction is 1.07, 2.05 and 2.36 MPa for $v = 1$, 2 and 3 mm/min, respectively. Obviously, the average normal stress gradually increases by 91.1% for v from 1 to 2 mm/min and by 14.8% for v from 2 to 3 mm/min. The average normal displacement increases by 34.1% for v from 1 to 2 mm/min and by 15.5% for v from 2 to 3 mm/min.

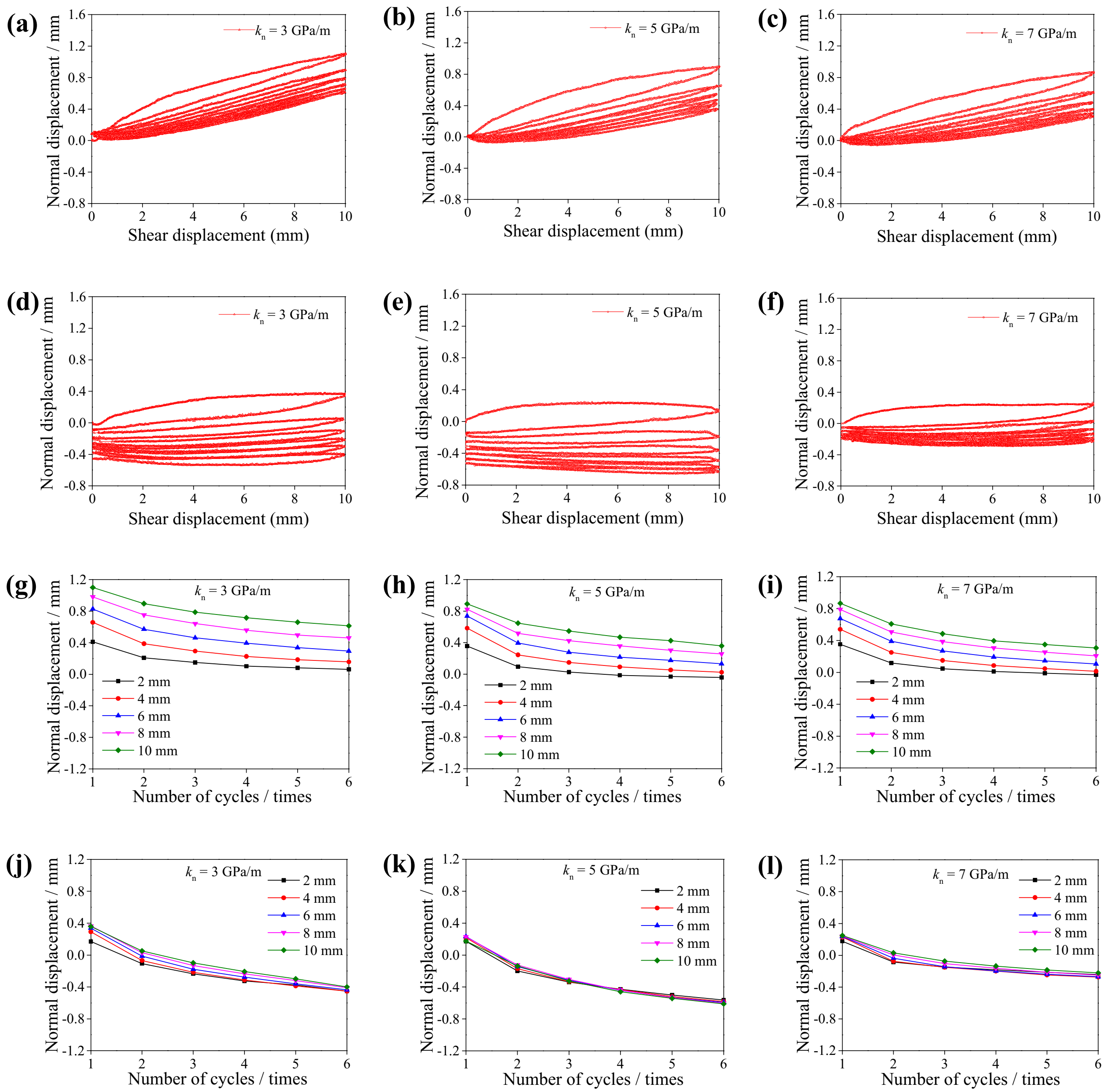

Fig. 10 **a–f** The variations in normal displacement with varying shear displacements of unfilled and infilled rock joints, respectively, under different k_n; **g–l** normal displacement versus number of cycles of unfilled and infilled rock joints, respectively, under different k_n

4 Empirical Models

Although a number of empirical models have been proposed to predict the mechanical behaviours of rock fractures during shearing by considering the CNL conditions (Oh et al. 2015; Li et al. 2016), the regular saw-toothed rock joints (Mirzaghorbanali et al. 2014), the monotonic loading under CNS conditions (Indraratna et al. 2005; Indraratna et al. 2015), and so on (Seidel and Haberfield 2002; Li et al. 2018), there is still no predictive model to simultaneously take into account the effects of σ_{n0}, k_n, v, δ_h and N for both infilled and unfilled naturally rough rock joints. In this section, based on the above experimental results, we adopted a multi-variable regression algorithm to establish empirical relationships.

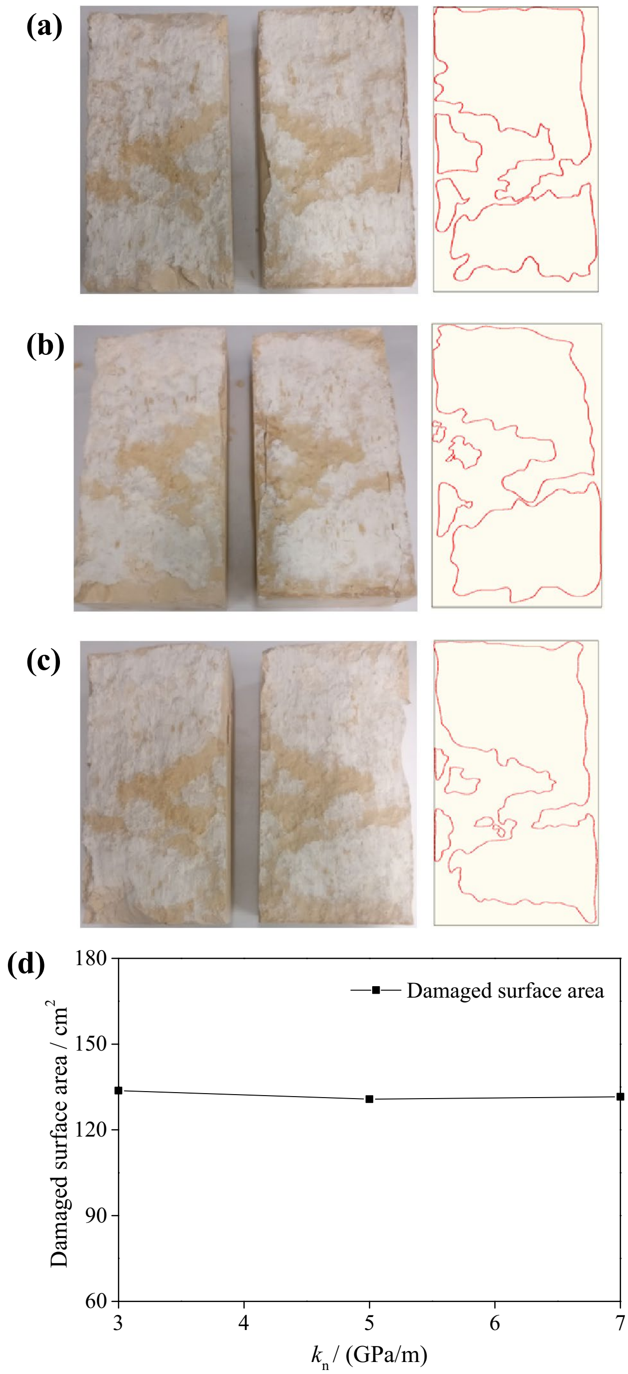

Fig. 11 Failure modes of unfilled rock joints under different k_n, **a** $k_n=3$ GPa/m, **b** $k_n=5$ GPa/m, **c** $k_n=7$ GPa/m, **d** damaged surface area vs. k_n

The shear stress, normal stress and normal displacement for both infilled and unfilled rock joints are independent variables, and σ_{n0}, k_n, v, δ_h and N are dependent variables. The cases and corresponding parameters used for fitting the regression functions are listed in "Appendix" (Table 1). The best-fitted expressions are as follows:

$$\tau_{\text{unfilled}} = 0.497\sigma_{n0} + 0.0964k_n + 0.1176v + 0.1251\delta_h - 0.1525N + 0.023, \quad (6)$$

$$\sigma_{n(\text{unfilled})} = 1.1167\sigma_{n0} + 0.1543k_n + 0.3336v + 0.3107\delta_h - 0.4780N - 0.3611, \quad (7)$$

$$\delta_{v(\text{unfilled})} = 0.0229\sigma_{n0} - 0.0473k_n + 0.0568v + 0.0635\delta_h - 0.0962N + 0.3437, \quad (8)$$

$$\tau_{\text{infilled}} = \exp(0.1311\sigma_{n0} + 0.0066k_n + 0.0412v + 0.003\delta_h - 0.2558N + 0.5611), \quad (9)$$

$$\sigma_{n(\text{infilled})} = \exp(0.1384\sigma_{n0} - 0.0103k_n + 0.0485v + 0.0078\delta_h - 0.233N + 1.1847), \quad (10)$$

$$\delta_{v(\text{infilled})} = -0.1271\sigma_{n0} + 0.015k_n + 0.0403v + 0.0054\delta_h - 0.1267N + 0.5758, \quad (11)$$

where τ_{unfilled}, $\sigma_{n(\text{unfilled})}$ and $\delta_{v(\text{unfilled})}$ are the shear stress, normal stress and normal displacement of unfilled rock joints, and τ_{infilled}, $\sigma_{n(\text{infilled})}$ and $\delta_{v(\text{infilled})}$ are the shear stress, normal stress and normal displacement of infilled rock joints.

For unfilled rock joints, τ_{unfilled} and $\sigma_{n(\text{unfilled})}$ are positively correlated with σ_{n0}, k_n, v and δ_h (see Fig. 16a, b), and the coefficient of σ_{n0} is significantly larger than those of other variables, as shown in Eqs. (6) and (7). This indicates that σ_{n0} plays the most significant role in τ_{unfilled} and $\sigma_{n(\text{unfilled})}$. However, the $\delta_{v(\text{unfilled})}$ is negatively correlated with k_n, as shown in Fig. 16c and Eq. (8). All of the τ_{unfilled}, $\sigma_{n(\text{unfilled})}$ and $\delta_{v(\text{unfilled})}$ are negatively correlated with N because the larger N results in a more significant degradation on the rough joint surfaces. For infilled rock joints, τ_{infilled} and $\sigma_{n(\text{infilled})}$ are expressed by exponential functions, which are positively correlated with σ_{n0}, v and δ_h, and negatively correlated with N (see Fig. 16d, e and Eqs. (9) and (10)). The $\delta_{v(\text{infilled})}$ is negatively correlated with σ_{n0} and N and positively correlated with k_n, v and δ_h (see Fig. 16f) and Eq. (11)). Equations (6–11) can accurately predict the variations in the shear stress, normal stress and normal displacement of both unfilled and infilled rock joints under cyclic loading and CNS conditions, in which the correlation coefficients R^2 are 0.781, 0.892, 0.827, 0.803, 0.824 and 0.782. Note that this is a primary work that aims to propose empirical models for calculating the mechanical behaviors of both

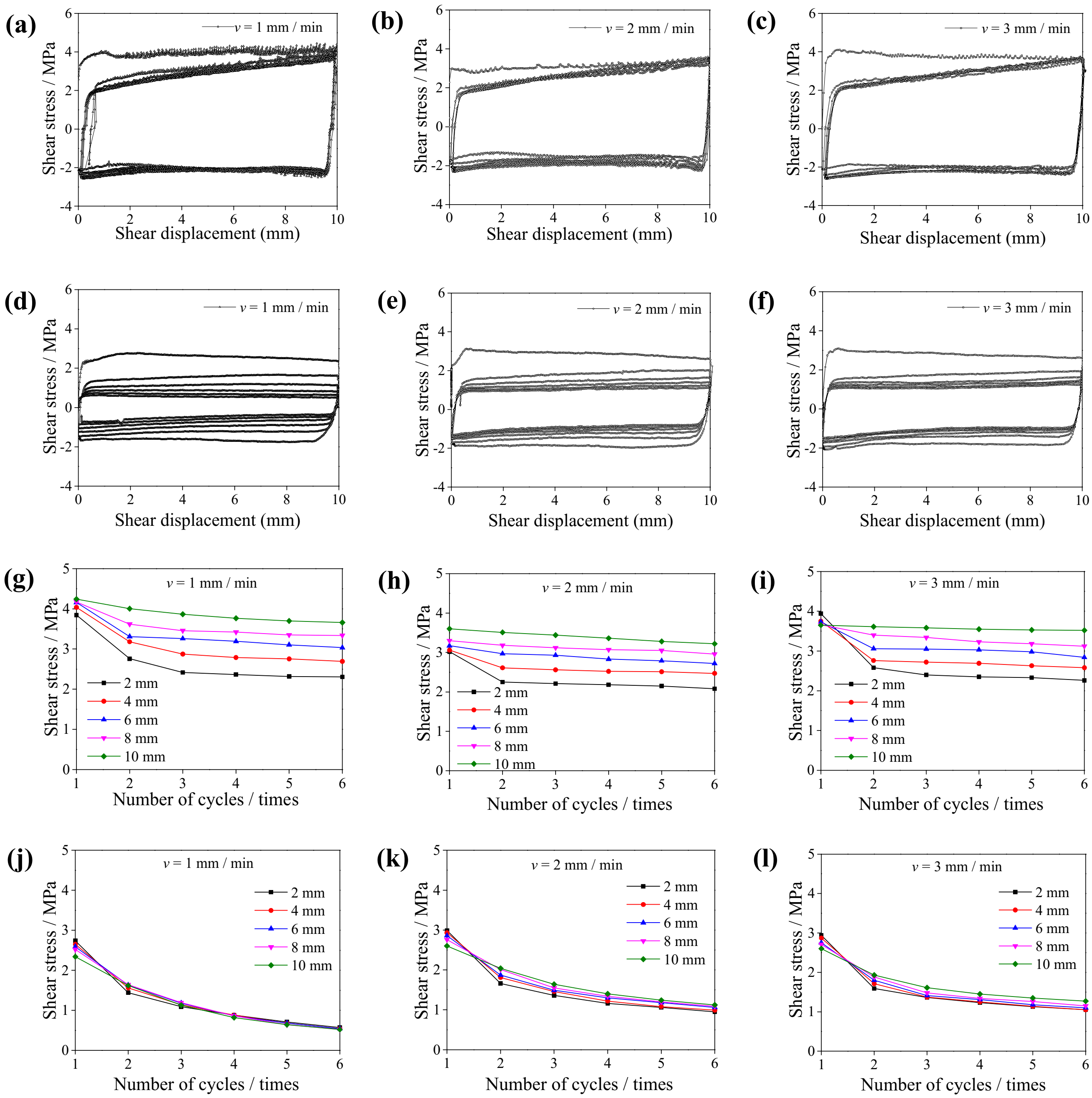

Fig. 12 **a–f** The variations in shear stress with varying shear displacements of unfilled and infilled rock joints, respectively, under different v; **g–l** shear stress versus number of cycles of unfilled and infilled rock joints, respectively, under different v

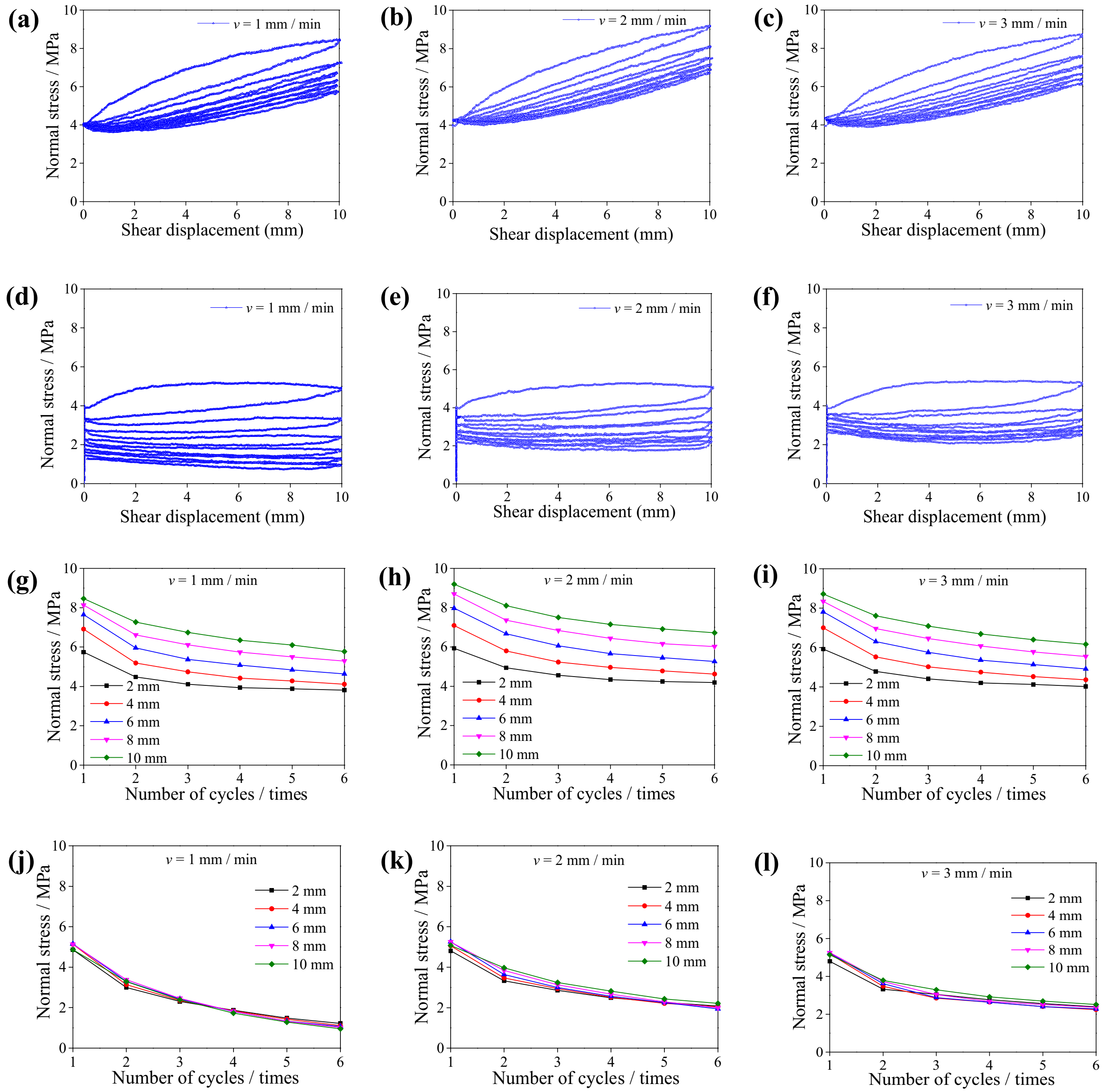

Fig. 13 **a–f** The variations in normal stress with varying shear displacements of unfilled and infilled rock joints, respectively, under different *v*; **g–l** normal stress versus number of cycles of unfilled and infilled rock joints, respectively, under different *v*

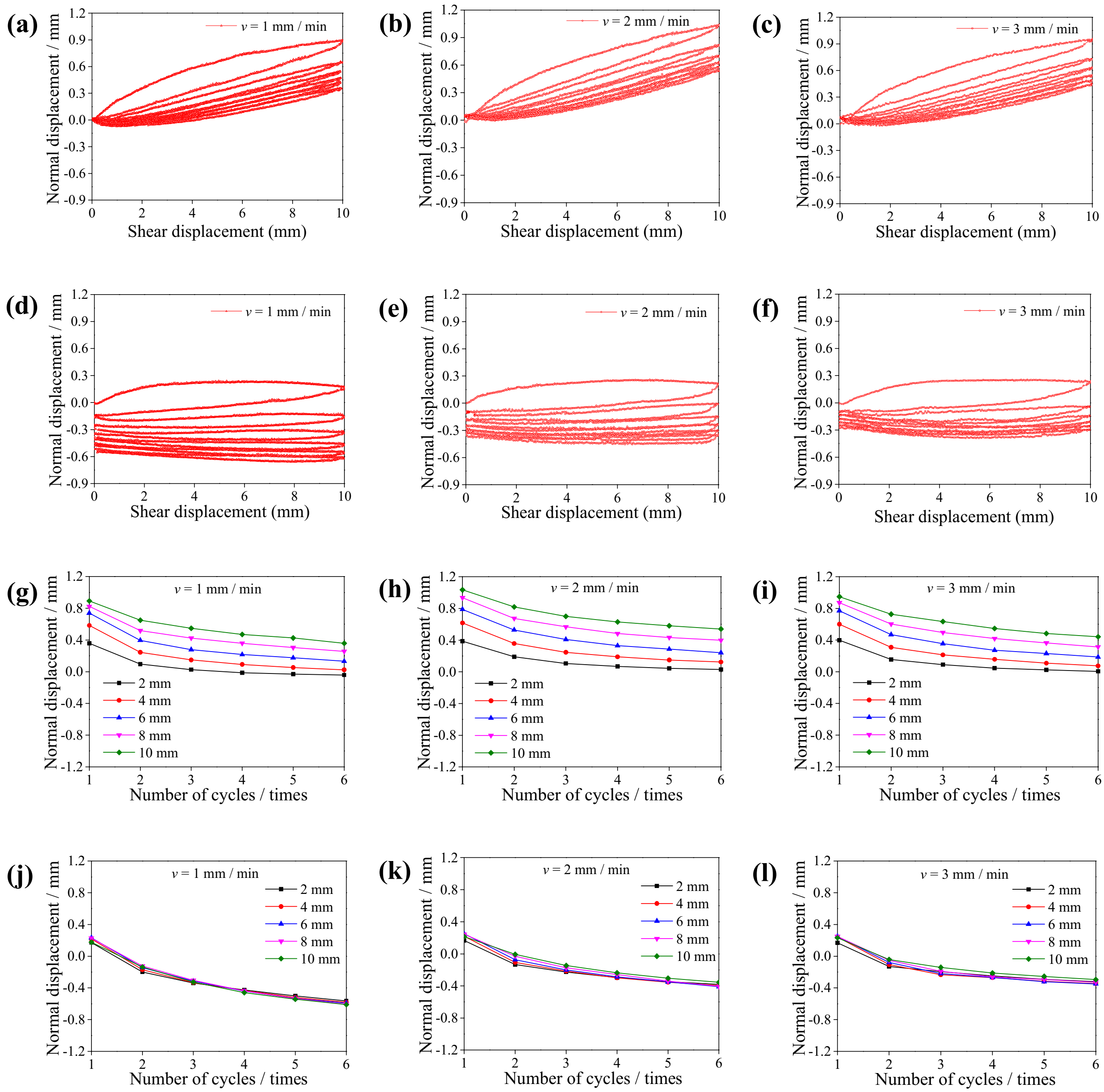

Fig. 14 **a–f** The variations in normal displacement with varying shear displacements of unfilled and infilled rock joints, respectively, under different *v*; **g–l** normal displacement versus number of cycles of unfilled and infilled rock joints, respectively, under different *v*

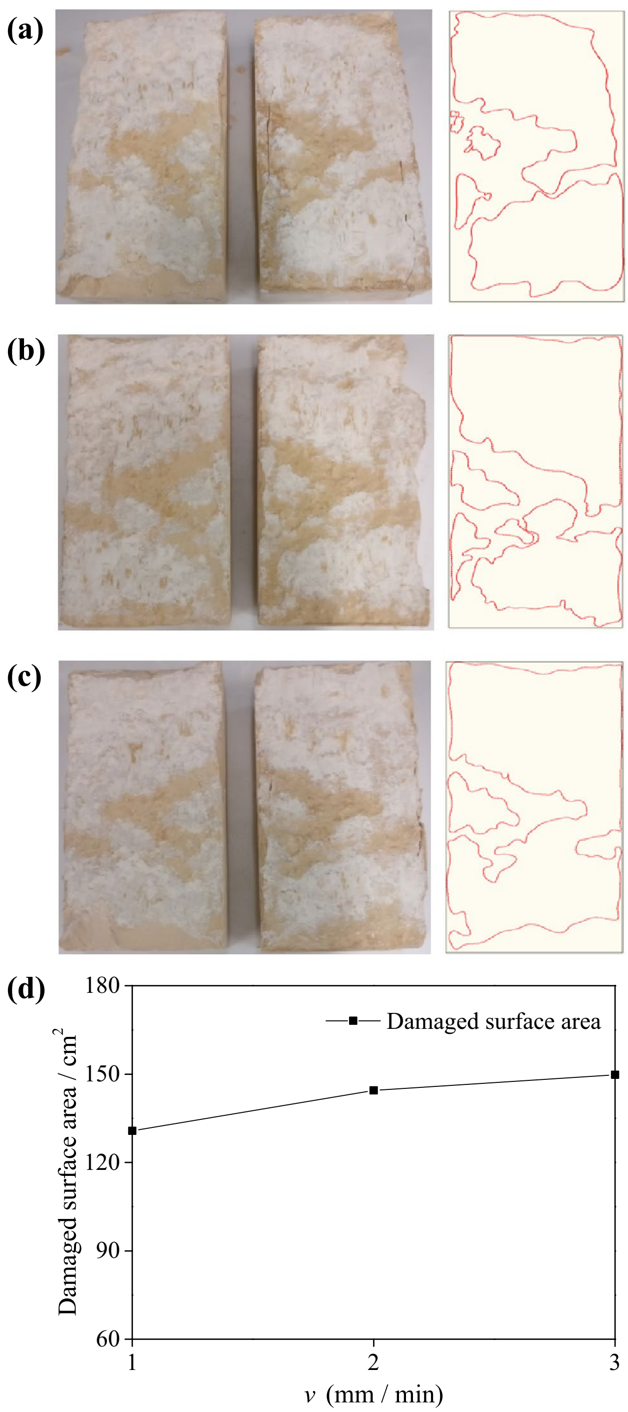

Fig. 15 Failure modes of unfilled rock joints under different v, **a** $v=1$ mm/min, **b** $v=2$ mm/min, **c** $v=3$ mm/min, **d** damaged surface area vs. v

infilled and unfilled rock joints under cyclic loading and CNS conditions. In the future works, we will facilitate these models by considering the influences of filling thickness, joint surface roughness, model size, and so on.

To quantitatively analyze the effect of fillings on the mechanical behaviours of rock joints, r_τ and r_σ are defined as follows:

$$r_\tau = \frac{\tau_{\text{unfilled}} - \tau_{\text{infilled}}}{\tau_{\text{unfilled}}} \times 100\%, \tag{12}$$

$$r_\sigma = \frac{\sigma_{n(\text{unfilled})} - \sigma_{n(\text{infilled})}}{\sigma_{n(\text{unfilled})}} \times 100\%, \tag{13}$$

where τ_{unfilled}, τ_{infilled}, $\sigma_{\text{n(unfilled)}}$ and $\sigma_{\text{n(infilled)}}$ are the predicted results using Eqs. (6), (7), (9) and (10), and the variations in r_τ and r_σ under different cases are displayed in Fig. 17a. The minimum, maximum and average values of r_τ are 24.96, 65.52 and 50.30%, respectively. The minimum, maximum and average values of r_σ are 9.38, 57.95 and 48.26%, respectively. The existence of fillings decreases the shear stress and normal stress by approximately 24.96–65.52% and 9.38–57.95%, respectively. Figure 17b shows the change in $\delta_{\text{v(unfilled)}} - \delta_{\text{v(infilled)}}$ for different cases, which depicts that the $\delta_{\text{v(unfilled)}}$ increases by 0.535 mm on average than $\delta_{\text{v(infilled)}}$. This is reasonable because the fillings have smaller strength values than the rocks, resulting in the damage in the fillings during shearing when the joints are filled. However, when the joints are unfilled, asperity degradation occurs during the shear-related dilation process and gives rise to a larger normal displacement than the infilled joints.

5 Conclusions

In this study, shear tests of unfilled and infilled rough rock joints under cyclic loading and CNS conditions were conducted. The influences of initial normal stress (σ_{n0}), normal stiffness (k_{n}) and shear velocity (v) on the shear behaviours, such as shear stress (τ), normal stress (σ_{n}) and normal displacement (δ_{v}), were estimated and analysed. Finally, empirical models were proposed to evaluate the variations in τ, σ_{n} and δ_{v} for the unfilled and infilled rock joints.

The results show that the τ, σ_{n} and δ_{v} for both unfilled and infilled rock joints decrease with the increase in the number of cycles (N), which show a rapid decline for $N=1$–2 and a

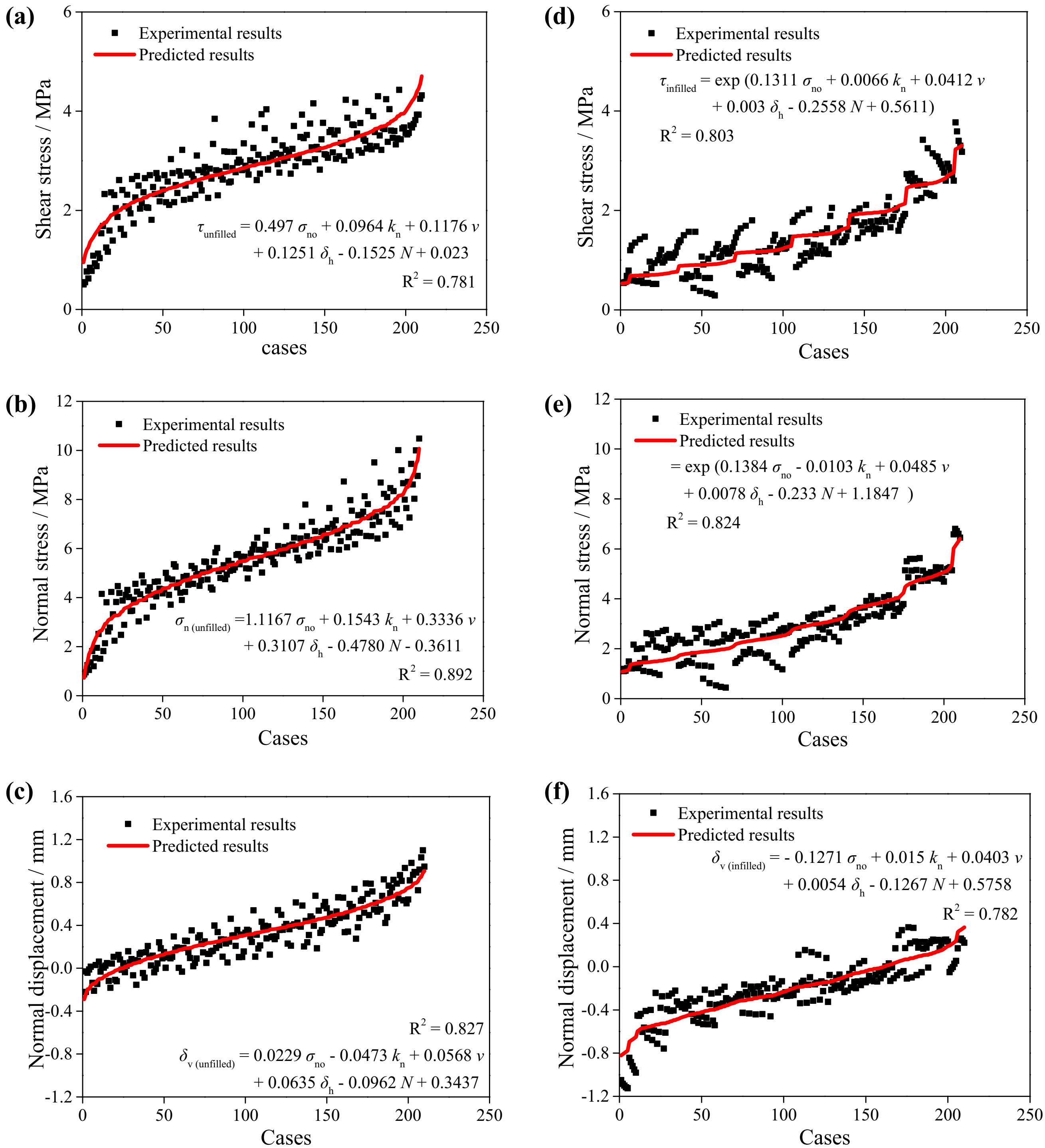

Fig. 16 Experimental results and predicted results for shear stress, normal stress and normal displacement of unfilled (**a**–**c** the left column) and infilled (**d**–**f** the right column) rock joints, respectively

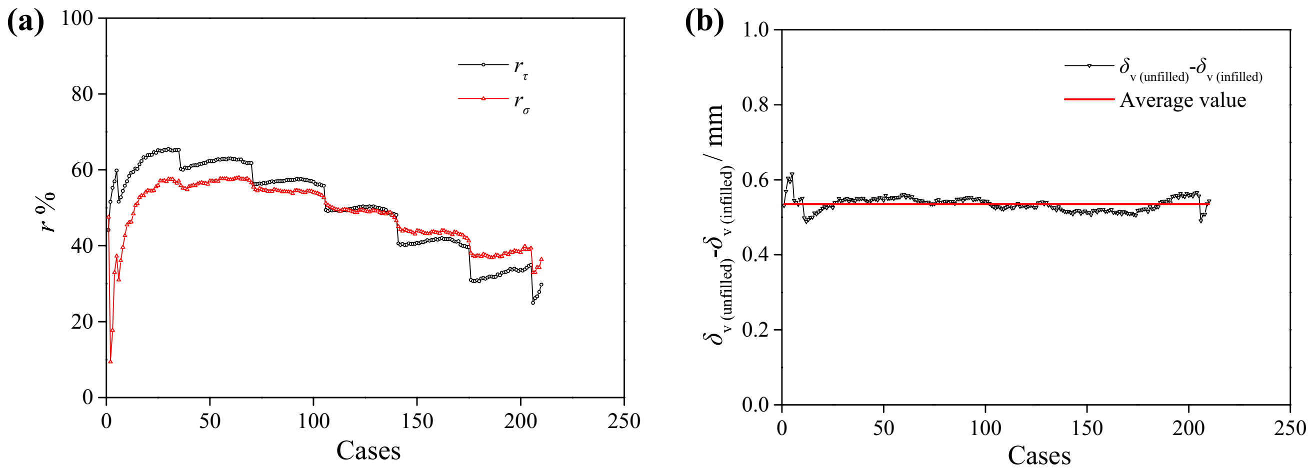

Fig. 17 Comparisons of mechanical behaviors during shearing for unfilled and infilled rock joints: **a** the shear stress and normal stress, and **b** the normal displacement

slow decline for $N=2$–6. Taking the unfilled rock joints as an example, the shear stress decreases by 51.4% for N from 1 to 2 and by 36.0% for N from 2 to 6, respectively, when $\sigma_{n0}=2$ MPa, $k_n=5$ GP/m, $v=1$ mm/min and $\delta_h=2$ mm. Since the density and uniaxial compressive strength of the filling materials are smaller than those of rock-like materials, the filling materials play a priority role during shearing. The τ and σ_n of unfilled rock joints are larger than those of infilled rock joints by approximately 24.96–65.52% and 9.38–57.95%, respectively, and the $\delta_{v(unfilled)}$ increases by 0.535 mm on average than $\delta_{v(infilled)}$. For unfilled rock joints, the damaged area increases by a rate of 52.5% for σ_{n0} increasing from 2 to 4 MPa and increases by a rate of 7% for σ_{n0} increasing from 4 to 6 MPa. However, the damaged area increases slightly with increases in v and k_n. The variations in the damaged area indicate that σ_{n0} plays a more significant role in the shear tests of rock joints than k_n and v. Six empirical models for predicting τ, σ_n and δ_v of unfilled and infilled rock joints under cyclic loading and CNS conditions are proposed, and the experimental results agree well with the predicted results, in which the correlation coefficients for all cases are larger than 0.78.

In the present study, the effects of cyclic loading and fillings on the shear behaviours of rough rock joints under CNS conditions have been deeply analysed, and six empirical functions have been proposed to predict the shear behaviours of both unfilled and infilled joints. However, the specimens have only one surface morphology with a unique JRC value, and the influence of height of the filling height has not been estimated. In future works, we will facilitate predictive models of the mechanical behaviours of rough joints during cyclic shearing under CNS conditions using rock joints that have different surface roughness, heights and mechanical properties of infilling materials.

Acknowledgements This study is partially funded by the National Natural Science Foundation of China (Grant nos. 51734009 and 51709260), and Natural Science Foundation of Jiangsu Province, China (Grant no. BK20170276).

Compliance with ethical standards

Conflict of interest The authors declare that they have no conflict of interest.

Appendix

See Table 1.

Table 1 The values of σ_{n0}, k_n, v, δ_h, and N used in the fitting curves, and experimental results and predicted results of τ, σ_n and δ_v

No.	σ_{n0}	k_n	v	δ_h	N	E: $\tau_{unfilled}$	P: $\tau_{unfilled}$	E: $\sigma_{n(unfilled)}$	P: $\sigma_{n(unfilled)}$	E: $\delta_{v(unfilled)}$	P: $\delta_{v(unfilled)}$	E: $\tau_{infilled}$	P: $\tau_{infilled}$	E: $\sigma_{n(infilled)}$	P: $\sigma_{n(infilled)}$	E: $\delta_{v(infilled)}$	P: $\delta_{v(infilled)}$
1	2	5	1	2	1	1.683	1.715	2.780	3.121	0.163	0.241	1.770	1.911	2.860	3.459	0.170	0.321
2	2	5	1	4	1	1.868	1.965	3.470	3.742	0.299	0.368	1.780	1.922	3.260	3.514	0.250	0.332
3	2	5	1	6	1	2.034	2.215	4.170	4.364	0.442	0.495	1.700	1.934	3.320	3.569	0.259	0.343
4	2	5	1	8	1	2.163	2.466	4.710	4.985	0.550	0.622	1.620	1.945	3.280	3.625	0.244	0.353
5	2	5	1	10	1	2.303	2.716	5.180	5.607	0.641	0.749	1.530	1.957	3.170	3.682	0.222	0.364
6	2	5	1	2	2	0.874	1.562	1.510	2.643	0.093	0.144	0.860	1.480	1.770	2.740	− 0.050	0.194
7	2	5	1	4	2	1.164	1.813	2.240	3.264	0.053	0.271	0.910	1.488	1.950	2.783	− 0.020	0.205
8	2	5	1	6	2	1.508	2.063	3.030	3.886	0.210	0.398	0.990	1.497	2.000	2.827	− 0.004	0.216
9	2	5	1	8	2	1.808	2.313	3.710	4.507	0.342	0.525	1.070	1.506	2.130	2.871	0.028	0.227
10	2	5	1	10	2	2.232	2.564	4.330	5.129	0.476	0.652	1.140	1.515	2.300	2.916	0.054	0.237
11	2	5	1	2	3	0.779	1.410	1.200	2.165	− 0.155	0.048	0.720	1.146	1.430	2.170	− 0.110	0.068
12	2	5	1	4	3	1.037	1.660	1.820	2.786	− 0.032	0.175	0.700	1.152	1.510	2.205	− 0.100	0.078
13	2	5	1	6	3	1.391	1.911	2.480	3.408	0.105	0.302	0.770	1.159	1.610	2.239	− 0.078	0.089
14	2	5	1	8	3	1.734	2.161	3.180	4.029	0.243	0.429	0.860	1.166	1.780	2.274	− 0.052	0.100
15	2	5	1	10	3	2.164	2.411	3.900	4.651	0.381	0.556	0.990	1.173	1.980	2.310	− 0.009	0.111
16	2	5	1	2	4	0.626	1.257	1.050	1.687	− 0.183	− 0.048	0.630	0.887	1.320	1.719	− 0.136	− 0.059
17	2	5	1	4	4	0.931	1.508	1.540	2.309	− 0.088	0.079	0.620	0.892	1.350	1.746	− 0.130	− 0.048
18	2	5	1	6	4	1.250	1.758	2.140	2.930	0.049	0.206	0.660	0.898	1.390	1.774	− 0.129	− 0.037
19	2	5	1	8	4	1.625	2.008	2.890	3.551	0.184	0.333	0.780	0.903	1.510	1.802	− 0.108	− 0.027
20	2	5	1	10	4	2.063	2.259	3.630	4.173	0.330	0.460	0.910	0.908	1.780	1.830	− 0.047	− 0.016
21	2	5	1	2	5	0.551	1.105	0.950	1.209	− 0.210	− 0.144	0.590	0.687	1.260	1.362	− 0.149	− 0.186
22	2	5	1	4	5	0.841	1.355	1.360	1.831	− 0.121	− 0.017	0.580	0.691	1.210	1.383	− 0.167	− 0.175
23	2	5	1	6	5	1.128	1.606	1.950	2.452	− 0.006	0.110	0.590	0.695	1.230	1.405	− 0.163	− 0.164
24	2	5	1	8	5	1.593	1.856	2.620	3.073	0.134	0.237	0.710	0.699	1.420	1.427	− 0.137	− 0.153
25	2	5	1	10	5	2.036	2.106	3.450	3.695	0.296	0.364	0.840	0.703	1.600	1.449	− 0.077	− 0.143
26	2	5	1	2	6	0.507	0.952	0.870	0.731	− 0.221	− 0.241	0.550	0.532	1.190	1.079	− 0.165	− 0.312
27	2	5	1	4	6	0.767	1.203	1.250	1.353	− 0.146	− 0.114	0.540	0.535	1.100	1.096	− 0.184	− 0.302
28	2	5	1	6	6	1.085	1.453	1.820	1.974	− 0.037	0.013	0.560	0.538	1.120	1.113	− 0.185	− 0.291
29	2	5	1	8	6	1.539	1.703	2.520	2.595	0.102	0.140	0.680	0.541	1.220	1.130	− 0.162	− 0.280
30	2	5	1	10	6	2.045	1.954	3.320	3.217	0.267	0.267	0.790	0.545	1.490	1.148	− 0.110	− 0.269
31	4	5	1	2	1	3.845	2.709	5.740	5.354	0.357	0.286	2.740	2.484	4.860	4.563	0.172	0.067
32	4	5	1	4	1	4.037	2.960	6.910	5.976	0.584	0.413	2.650	2.499	5.130	4.634	0.218	0.078
33	4	5	1	6	1	4.159	3.210	7.650	6.597	0.739	0.540	2.590	2.513	5.150	4.707	0.232	0.088
34	4	5	1	8	1	4.171	3.460	8.130	7.219	0.823	0.667	2.520	2.528	5.130	4.781	0.228	0.099
35	4	5	1	10	1	4.240	3.710	8.460	7.840	0.893	0.794	2.340	2.543	4.870	4.856	0.176	0.110
36	4	5	1	2	2	2.758	2.557	4.480	4.876	0.095	0.190	1.440	1.923	3.000	3.614	− 0.199	− 0.060
37	4	5	1	4	2	3.180	2.807	5.190	5.498	0.245	0.317	1.560	1.935	3.140	3.671	− 0.170	− 0.049

Table 1 (continued)

No.	σ_{n0}	k_n	v	δ_h	N	E: $\tau_{unfilled}$	P: $\tau_{unfilled}$	E: $\sigma_{n(unfilled)}$	P: $\sigma_{n(unfilled)}$	E: $\delta_{v(unfilled)}$	P: $\delta_{v(unfilled)}$	E: $\tau_{infilled}$	P: $\tau_{infilled}$	E: $\sigma_{n(infilled)}$	P: $\sigma_{n(infilled)}$	E: $\delta_{v(infilled)}$	P: $\delta_{v(infilled)}$
38	4	5	1	6	2	3.309	3.057	5.960	6.119	0.395	0.444	1.630	1.946	3.300	3.729	− 0.143	− 0.038
39	4	5	1	8	2	3.618	3.308	6.620	6.741	0.518	0.571	1.640	1.958	3.380	3.787	− 0.124	− 0.028
40	4	5	1	10	2	4.002	3.558	7.270	7.362	0.649	0.698	1.620	1.969	3.290	3.847	− 0.137	− 0.017
41	4	5	1	2	3	2.415	2.404	4.110	4.398	0.026	0.094	1.090	1.489	2.300	2.863	− 0.338	− 0.187
42	4	5	1	4	3	2.874	2.655	4.740	5.020	0.148	0.221	1.140	1.498	2.350	2.908	− 0.334	− 0.176
43	4	5	1	6	3	3.259	2.905	5.370	5.641	0.278	0.348	1.180	1.507	2.430	2.954	− 0.315	− 0.165
44	4	5	1	8	3	3.457	3.155	6.110	6.263	0.424	0.475	1.190	1.516	2.460	3.000	− 0.305	− 0.154
45	4	5	1	10	3	3.866	3.406	6.740	6.884	0.547	0.602	1.130	1.525	2.390	3.047	− 0.325	− 0.144
46	4	5	1	2	4	2.365	2.252	3.940	3.920	− 0.014	− 0.002	0.880	1.153	1.870	2.268	− 0.427	− 0.313
47	4	5	1	4	4	2.788	2.502	4.420	4.542	0.092	0.125	0.880	1.160	1.840	2.303	− 0.433	− 0.303
48	4	5	1	6	4	3.191	2.752	5.080	5.163	0.216	0.252	0.860	1.167	1.800	2.340	− 0.441	− 0.292
49	4	5	1	8	4	3.420	3.003	5.740	5.785	0.358	0.379	0.860	1.174	1.810	2.376	− 0.439	− 0.281
50	4	5	1	10	4	3.763	3.253	6.350	6.406	0.470	0.506	0.820	1.181	1.730	2.414	− 0.459	− 0.270
51	4	5	1	2	5	2.315	2.099	3.880	3.442	− 0.031	− 0.099	0.710	0.893	1.480	1.796	− 0.501	− 0.440
52	4	5	1	4	5	2.752	2.350	4.280	4.064	0.053	0.028	0.680	0.898	1.430	1.824	− 0.519	− 0.429
53	4	5	1	6	5	3.104	2.600	4.840	4.685	0.175	0.155	0.680	0.903	1.330	1.853	− 0.532	− 0.418
54	4	5	1	8	5	3.350	2.850	5.500	5.307	0.304	0.282	0.640	0.909	1.320	1.882	− 0.534	− 0.408
55	4	5	1	10	5	3.700	3.101	6.100	5.928	0.425	0.409	0.640	0.914	1.280	1.912	− 0.542	− 0.397
56	4	5	1	2	6	2.306	1.947	3.810	2.964	− 0.042	− 0.195	0.570	0.691	1.220	1.423	− 0.564	− 0.567
57	4	5	1	4	6	2.690	2.197	4.110	3.586	0.024	− 0.068	0.540	0.695	1.110	1.445	− 0.582	− 0.556
58	4	5	1	6	6	3.034	2.447	4.640	4.207	0.132	0.059	0.540	0.699	1.070	1.468	− 0.591	− 0.545
59	4	5	1	8	6	3.337	2.698	5.290	4.829	0.257	0.186	0.520	0.704	1.020	1.491	− 0.604	− 0.534
60	4	5	1	10	6	3.657	2.948	5.770	5.450	0.358	0.313	0.520	0.708	0.950	1.514	− 0.611	− 0.524
61	6	5	1	2	1	3.640	3.704	7.510	7.588	0.313	0.332	3.770	3.228	6.580	6.018	0.110	− 0.187
62	6	5	1	4	1	3.670	3.954	8.660	8.209	0.538	0.459	3.590	3.247	6.800	6.113	0.154	− 0.177
63	6	5	1	6	1	3.670	4.204	9.450	8.831	0.694	0.586	3.400	3.267	6.710	6.209	0.134	− 0.166
64	6	5	1	8	1	3.930	4.455	10.000	9.452	0.815	0.713	3.300	3.286	6.600	6.306	0.110	− 0.155
65	6	5	1	10	1	4.320	4.705	10.480	10.074	0.920	0.840	3.180	3.306	6.450	6.406	0.080	− 0.144
66	6	5	1	2	2	3.244	3.551	6.640	7.110	0.134	0.236	2.200	2.500	4.710	4.767	− 0.267	− 0.314
67	6	5	1	4	2	3.460	3.802	7.410	7.731	0.290	0.363	2.250	2.514	4.720	4.842	− 0.261	− 0.303
68	6	5	1	6	2	3.530	4.052	7.990	8.353	0.411	0.490	2.350	2.529	4.820	4.918	− 0.247	− 0.293
69	6	5	1	8	2	3.820	4.302	8.610	8.974	0.528	0.617	2.310	2.545	4.820	4.995	− 0.243	− 0.282
70	6	5	1	10	2	4.250	4.552	8.960	9.596	0.605	0.744	2.290	2.560	4.690	5.074	− 0.274	− 0.271
71	6	5	1	2	3	3.010	3.399	5.970	6.632	0.004	0.140	1.760	1.935	3.870	3.776	− 0.437	− 0.441
72	6	5	1	4	3	3.290	3.649	6.510	7.253	0.107	0.267	1.780	1.947	3.780	3.835	− 0.455	− 0.430
73	6	5	1	6	3	3.450	3.899	7.090	7.875	0.229	0.394	1.790	1.959	3.690	3.896	− 0.462	− 0.419

Table 1 (continued)

No.	σ_{n0}	k_n	v	δ_h	N	E: $\tau_{unfilled}$	P: $\tau_{unfilled}$	E: $\sigma_{n(unfilled)}$	P: $\sigma_{n(unfilled)}$	E: $\delta_{v(unfilled)}$	P: $\delta_{v(unfilled)}$	E: $\tau_{infilled}$	P: $\tau_{infilled}$	E: $\sigma_{n(infilled)}$	P: $\sigma_{n(infilled)}$	E: $\delta_{v(infilled)}$	P: $\delta_{v(infilled)}$
74	6	5	1	8	3	3.710	4.150	7.650	8.496	0.336	0.521	1.810	1.970	3.660	3.957	− 0.473	− 0.409
75	6	5	1	10	3	3.930	4.400	8.030	9.118	0.422	0.648	1.770	1.982	3.590	4.019	− 0.500	− 0.398
76	6	5	1	2	4	2.820	3.246	5.620	6.154	− 0.066	0.043	1.370	1.499	3.010	2.991	− 0.604	− 0.568
77	6	5	1	4	4	3.210	3.497	5.950	6.775	0.003	0.170	1.310	1.507	2.770	3.038	− 0.659	− 0.557
78	6	5	1	6	4	3.380	3.747	6.500	7.397	0.104	0.297	1.290	1.516	2.650	3.086	− 0.679	− 0.546
79	6	5	1	8	4	3.560	3.997	6.970	8.018	0.203	0.424	1.210	1.525	2.470	3.134	− 0.713	− 0.535
80	6	5	1	10	4	3.740	4.247	7.260	8.640	0.275	0.551	1.120	1.535	2.290	3.184	− 0.758	− 0.525
81	6	5	1	2	5	2.740	3.094	5.510	5.676	− 0.119	− 0.053	0.850	1.160	1.860	2.369	− 0.843	− 0.694
82	6	5	1	4	5	3.040	3.344	5.680	6.297	− 0.046	0.074	0.810	1.167	1.630	2.406	− 0.884	− 0.683
83	6	5	1	6	5	3.230	3.594	6.050	6.919	0.019	0.201	0.760	1.174	1.440	2.444	− 0.919	− 0.673
84	6	5	1	8	5	3.330	3.845	6.410	7.540	0.108	0.328	0.690	1.181	1.270	2.483	− 0.953	− 0.662
85	6	5	1	10	5	3.560	4.095	6.860	8.162	0.186	0.455	0.640	1.188	1.170	2.522	− 0.981	− 0.651
86	6	5	1	2	6	2.740	2.941	5.320	5.198	− 0.137	− 0.149	0.440	0.898	0.800	1.877	− 1.050	− 0.821
87	6	5	1	4	6	2.970	3.192	5.450	5.819	− 0.109	− 0.022	0.380	0.904	0.620	1.906	− 1.085	− 0.810
88	6	5	1	6	6	3.100	3.442	5.800	6.441	− 0.038	0.105	0.340	0.909	0.530	1.936	− 1.100	− 0.799
89	6	5	1	8	6	3.220	3.692	6.170	7.062	0.050	0.232	0.320	0.915	0.470	1.967	− 1.116	− 0.789
90	6	5	1	10	6	3.430	3.942	6.560	7.684	0.127	0.359	0.290	0.920	0.440	1.998	− 1.125	− 0.778
91	4	3	1	2	1	3.220	2.516	5.200	5.046	0.412	0.381	2.730	2.451	4.460	4.658	0.170	0.037
92	4	3	1	4	1	3.180	2.767	5.950	5.667	0.658	0.508	2.650	2.466	4.830	4.731	0.292	0.047
93	4	3	1	6	1	3.150	3.017	6.500	6.289	0.828	0.635	2.600	2.480	5.000	4.805	0.338	0.058
94	4	3	1	8	1	3.130	3.267	6.930	6.910	0.982	0.762	2.580	2.495	5.050	4.881	0.365	0.069
95	4	3	1	10	1	3.160	3.518	7.310	7.532	1.100	0.889	2.500	2.510	5.090	4.958	0.359	0.080
96	4	3	1	2	2	2.640	2.364	4.610	4.568	0.209	0.285	1.780	1.898	3.650	3.690	− 0.107	− 0.090
97	4	3	1	4	2	2.810	2.614	5.150	5.189	0.388	0.412	1.900	1.909	3.760	3.748	− 0.068	− 0.079
98	4	3	1	6	2	2.900	2.865	5.680	5.811	0.571	0.539	1.970	1.921	3.940	3.806	− 0.013	− 0.068
99	4	3	1	8	2	2.890	3.115	6.230	6.432	0.753	0.666	2.040	1.932	4.070	3.866	0.030	− 0.058
100	4	3	1	10	2	3.090	3.365	6.650	7.054	0.897	0.793	2.110	1.943	4.140	3.927	0.052	− 0.047
101	4	3	1	2	3	2.500	2.212	4.420	4.090	0.149	0.188	1.770	1.470	3.250	2.923	− 0.235	− 0.217
102	4	3	1	4	3	2.750	2.462	4.880	4.711	0.295	0.315	1.810	1.478	3.310	2.968	− 0.215	− 0.206
103	4	3	1	6	3	2.810	2.712	5.370	5.333	0.463	0.442	1.900	1.487	3.400	3.015	− 0.177	− 0.195
104	4	3	1	8	3	2.820	2.962	5.920	5.954	0.643	0.569	1.950	1.496	3.560	3.063	− 0.131	− 0.184
105	4	3	1	10	3	3.030	3.213	6.350	6.576	0.789	0.696	2.020	1.505	3.630	3.111	− 0.098	− 0.174
106	4	3	1	2	4	2.410	2.059	4.310	3.612	0.103	0.092	1.460	1.138	3.000	2.315	− 0.326	− 0.343
107	4	3	1	4	4	2.710	2.309	4.660	4.233	0.227	0.219	1.550	1.145	3.000	2.351	− 0.313	− 0.333
108	4	3	1	6	4	2.760	2.560	5.190	4.855	0.395	0.346	1.640	1.151	3.110	2.388	− 0.277	− 0.322
109	4	3	1	8	4	2.770	2.810	5.670	5.476	0.559	0.473	1.690	1.158	3.240	2.426	− 0.236	− 0.311

Table 1 (continued)

No.	σ_{n0}	k_n	v	δ_h	N	E: $\tau_{unfilled}$	P: $\tau_{unfilled}$	E: $\sigma_{n(unfilled)}$	P: $\sigma_{n(unfilled)}$	E: $\delta_{v(unfilled)}$	P: $\delta_{v(unfilled)}$	E: $\tau_{infilled}$	P: $\tau_{infilled}$	E: $\sigma_{n(infilled)}$	P: $\sigma_{n(infilled)}$	E: $\delta_{v(infilled)}$	P: $\delta_{v(infilled)}$
110	4	3	1	10	4	3.000	3.060	6.110	6.098	0.716	0.600	1.800	1.165	3.340	2.464	− 0.206	− 0.300
111	4	3	1	2	5	2.360	1.907	4.230	3.134	0.082	− 0.004	1.360	0.881	2.800	1.834	− 0.375	− 0.470
112	4	3	1	4	5	2.630	2.157	4.560	3.755	0.186	0.123	1.400	0.886	2.790	1.863	− 0.387	− 0.459
113	4	3	1	6	5	2.710	2.407	5.010	4.377	0.338	0.250	1.500	0.892	2.860	1.892	− 0.362	− 0.448
114	4	3	1	8	5	2.730	2.657	5.470	4.998	0.498	0.377	1.570	0.897	2.980	1.922	− 0.321	− 0.438
115	4	3	1	10	5	2.960	2.908	5.960	5.620	0.661	0.504	1.570	0.902	3.070	1.952	− 0.298	− 0.427
116	4	3	1	2	6	2.330	1.754	4.150	2.656	0.062	− 0.100	1.200	0.682	2.620	1.453	− 0.452	− 0.597
117	4	3	1	4	6	2.610	2.004	4.470	3.277	0.158	0.027	1.290	0.686	2.580	1.475	− 0.454	− 0.586
118	4	3	1	6	6	2.650	2.255	4.900	3.899	0.295	0.154	1.350	0.690	2.620	1.499	− 0.437	− 0.575
119	4	3	1	8	6	2.700	2.505	5.360	4.520	0.461	0.281	1.420	0.694	2.710	1.522	− 0.410	− 0.564
120	4	3	1	10	6	2.880	2.755	5.840	5.142	0.614	0.408	1.470	0.699	2.750	1.546	− 0.400	− 0.554
121	4	7	1	2	1	3.730	2.902	6.440	5.663	0.353	0.192	3.420	2.517	5.140	4.469	0.177	0.097
122	4	7	1	4	1	3.930	3.152	7.790	6.284	0.540	0.319	3.250	2.532	5.500	4.540	0.228	0.108
123	4	7	1	6	1	4.230	3.403	8.730	6.906	0.676	0.446	3.150	2.547	5.600	4.611	0.236	0.118
124	4	7	1	8	1	4.300	3.653	9.510	7.527	0.791	0.573	3.090	2.562	5.600	4.683	0.240	0.129
125	4	7	1	10	1	4.430	3.903	10.010	8.149	0.868	0.700	3.080	2.577	5.630	4.757	0.248	0.140
126	4	7	1	2	2	2.620	2.750	4.800	5.185	0.117	0.096	1.680	1.949	3.330	3.540	− 0.086	− 0.030
127	4	7	1	4	2	3.120	3.000	5.760	5.806	0.250	0.223	1.770	1.960	3.390	3.596	− 0.075	− 0.019
128	4	7	1	6	2	3.430	3.250	6.710	6.428	0.390	0.350	1.940	1.972	3.640	3.652	− 0.036	− 0.008
129	4	7	1	8	2	3.760	3.501	7.540	7.049	0.507	0.477	2.100	1.984	3.910	3.710	0.003	0.002
130	4	7	1	10	2	4.040	3.751	8.230	7.671	0.609	0.604	2.270	1.996	4.100	3.768	0.030	0.013
131	4	7	1	2	3	2.310	2.597	4.230	4.707	0.046	− 0.001	1.520	1.509	2.870	2.804	− 0.148	− 0.157
132	4	7	1	4	3	2.810	2.847	5.090	5.328	0.150	0.126	1.560	1.518	2.840	2.848	− 0.150	− 0.146
133	4	7	1	6	3	3.240	3.098	5.930	5.950	0.270	0.253	1.640	1.527	2.940	2.893	− 0.143	-0.135
134	4	7	1	8	3	3.610	3.348	6.710	6.571	0.386	0.380	1.890	1.536	3.180	2.939	-0.105	− 0.124
135	4	7	1	10	3	3.900	3.598	7.370	7.193	0.484	0.507	2.050	1.545	3.370	2.985	− 0.073	− 0.114
136	4	7	1	2	4	2.110	2.445	4.050	4.229	0.011	− 0.097	1.170	1.168	2.640	2.221	− 0.183	− 0.283
137	4	7	1	4	4	2.640	2.695	4.560	4.851	0.085	0.030	1.180	1.175	2.510	2.256	− 0.200	− 0.272
138	4	7	1	6	4	3.030	2.945	5.360	5.472	0.193	0.157	1.240	1.182	2.550	2.292	− 0.197	− 0.262
139	4	7	1	8	4	3.270	3.196	6.120	6.093	0.307	0.284	1.390	1.189	2.720	2.328	− 0.164	− 0.251
140	4	7	1	10	4	3.720	3.446	6.800	6.715	0.396	0.411	1.510	1.196	2.970	2.364	− 0.135	− 0.240
141	4	7	1	2	5	2.050	2.292	3.910	3.751	− 0.012	− 0.193	1.070	0.905	2.360	1.760	− 0.214	− 0.410
142	4	7	1	4	5	2.500	2.542	4.330	4.373	0.047	− 0.066	1.030	0.910	2.220	1.787	− 0.248	− 0.399
143	4	7	1	6	5	2.850	2.793	5.030	4.994	0.145	0.061	1.120	0.915	2.240	1.815	− 0.238	− 0.388
144	4	7	1	8	5	3.120	3.043	5.800	5.615	0.254	0.188	1.230	0.921	2.430	1.844	− 0.214	− 0.378
145	4	7	1	10	5	3.580	3.293	6.410	6.237	0.350	0.315	1.320	0.926	2.600	1.873	− 0.186	− 0.367

Table 1 (continued)

No.	σ_{n0}	k_n	v	δ_h	N	E: $\tau_{unfilled}$	P: $\tau_{unfilled}$	E: $\sigma_{n(unfilled)}$	P: $\sigma_{n(unfilled)}$	E: $\delta_{v(unfilled)}$	P: $\delta_{v(unfilled)}$	E: $\tau_{infilled}$	P: $\tau_{infilled}$	E: $\sigma_{n(infilled)}$	P: $\sigma_{n(infilled)}$	E: $\delta_{v(infilled)}$	P: $\delta_{v(infilled)}$
146	4	7	1	2	6	1.940	2.140	3.820	3.273	− 0.030	− 0.289	0.970	0.700	2.160	1.394	− 0.242	− 0.537
147	4	7	1	4	6	2.330	2.390	4.140	3.895	0.014	− 0.162	0.940	0.705	1.990	1.416	− 0.274	− 0.526
148	4	7	1	6	6	2.770	2.640	4.740	4.516	0.106	− 0.035	1.000	0.709	2.010	1.438	− 0.269	− 0.515
149	4	7	1	8	6	3.010	2.891	5.480	5.137	0.207	0.092	1.100	0.713	2.170	1.461	− 0.249	− 0.504
150	4	7	1	10	6	3.480	3.141	6.160	5.759	0.307	0.219	1.210	0.717	2.330	1.483	− 0.222	− 0.494
151	4	5	2	2	1	3.020	2.827	5.930	5.688	0.386	0.343	2.990	2.588	4.810	4.789	0.167	0.107
152	4	5	2	4	1	3.060	3.077	7.090	6.309	0.617	0.470	2.930	2.604	5.060	4.865	0.219	0.118
153	4	5	2	6	1	3.170	3.328	7.970	6.931	0.788	0.597	2.860	2.619	5.260	4.941	0.250	0.129
154	4	5	2	8	1	3.300	3.578	8.690	7.552	0.935	0.724	2.760	2.635	5.250	5.019	0.245	0.139
155	4	5	2	10	1	3.600	3.828	9.190	8.174	1.034	0.851	2.600	2.650	5.080	5.098	0.214	0.150
156	4	5	2	2	2	2.250	2.674	4.940	5.210	0.189	0.247	1.660	2.004	3.330	3.794	− 0.134	− 0.020
157	4	5	2	4	2	2.610	2.925	5.800	5.831	0.357	0.374	1.810	2.016	3.470	3.853	− 0.107	− 0.009
158	4	5	2	6	2	2.970	3.175	6.670	6.453	0.529	0.501	1.870	2.028	3.640	3.914	− 0.074	0.002
159	4	5	2	8	2	3.180	3.425	7.360	7.074	0.674	0.628	2.010	2.040	3.840	3.975	− 0.029	0.013
160	4	5	2	10	2	3.510	3.676	8.100	7.696	0.819	0.755	2.040	2.052	3.970	4.038	− 0.007	0.023
161	4	5	2	2	3	2.210	2.522	4.560	4.732	0.106	0.151	1.360	1.552	2.860	3.005	− 0.226	− 0.146
162	4	5	2	4	3	2.560	2.772	5.230	5.353	0.247	0.278	1.460	1.561	2.940	3.052	− 0.214	− 0.135
163	4	5	2	6	3	2.930	3.023	6.060	5.975	0.409	0.405	1.490	1.570	3.000	3.100	− 0.200	− 0.125
164	4	5	2	8	3	3.120	3.273	6.840	6.596	0.568	0.532	1.550	1.579	3.130	3.149	− 0.174	− 0.114
165	4	5	2	10	3	3.440	3.523	7.500	7.218	0.700	0.659	1.640	1.589	3.240	3.198	− 0.146	− 0.103
166	4	5	2	2	4	2.180	2.369	4.340	4.254	0.068	0.054	1.160	1.201	2.490	2.380	− 0.296	− 0.273
167	4	5	2	4	4	2.520	2.620	4.960	4.875	0.189	0.181	1.220	1.209	2.520	2.418	− 0.298	− 0.262
168	4	5	2	6	4	2.830	2.870	5.660	5.497	0.330	0.308	1.300	1.216	2.560	2.456	− 0.288	− 0.251
169	4	5	2	8	4	3.070	3.120	6.440	6.118	0.483	0.435	1.340	1.223	2.670	2.494	− 0.258	− 0.241
170	4	5	2	10	4	3.360	3.371	7.150	6.740	0.629	0.562	1.399	1.230	2.820	2.534	− 0.237	− 0.230
171	4	5	2	2	5	2.150	2.217	4.240	3.776	0.044	− 0.042	1.060	0.930	2.260	1.886	− 0.346	− 0.400
172	4	5	2	4	5	2.510	2.467	4.780	4.397	0.149	0.085	1.080	0.936	2.210	1.915	− 0.354	− 0.389
173	4	5	2	6	5	2.790	2.718	5.450	5.019	0.286	0.212	1.180	0.941	2.250	1.945	− 0.350	− 0.378
174	4	5	2	8	5	3.050	2.968	6.160	5.640	0.433	0.339	1.200	0.947	2.290	1.976	− 0.340	− 0.367
175	4	5	2	10	5	3.280	3.218	6.910	6.262	0.581	0.466	1.240	0.953	2.430	2.007	− 0.304	− 0.357
176	4	5	2	2	6	2.080	2.064	4.190	3.298	0.030	− 0.138	0.950	0.720	2.080	1.494	− 0.381	− 0.526
177	4	5	2	4	6	2.470	2.315	4.620	3.919	0.124	− 0.011	0.990	0.725	2.040	1.517	− 0.394	− 0.516
178	4	5	2	6	6	2.720	2.565	5.260	4.541	0.241	0.116	1.060	0.729	1.940	1.541	− 0.410	− 0.505
179	4	5	2	8	6	2.960	2.815	6.020	5.162	0.398	0.243	1.090	0.733	1.990	1.565	− 0.405	− 0.494
180	4	5	2	10	6	3.220	3.066	6.720	5.784	0.541	0.370	1.120	0.738	2.210	1.590	− 0.354	− 0.483
181	4	5	3	2	1	3.940	2.945	5.920	6.022	0.397	0.400	2.940	2.697	4.800	5.027	0.169	0.147

Table 1 (continued)

No.	σ_{n0}	k_n	v	δ_h	N	E: $\tau_{unfilled}$	P: $\tau_{unfilled}$	E: $\sigma_{n(unfilled)}$	P: $\sigma_{n(unfilled)}$	E: $\delta_{v(unfilled)}$	P: $\delta_{v(unfilled)}$	E: $\tau_{infilled}$	P: $\tau_{infilled}$	E: $\sigma_{n(infilled)}$	P: $\sigma_{n(infilled)}$	E: $\delta_{v(infilled)}$	P: $\delta_{v(infilled)}$
182	4	5	3	4	1	3.750	3.195	7.000	6.643	0.600	0.527	2.870	2.713	5.190	5.106	0.240	0.158
183	4	5	3	6	1	3.730	3.445	7.810	7.264	0.770	0.654	2.750	2.729	5.230	5.187	0.249	0.169
184	4	5	3	8	1	3.660	3.695	8.340	7.886	0.871	0.781	2.710	2.745	5.260	5.268	0.250	0.180
185	4	5	3	10	1	3.650	3.946	8.720	8.507	0.948	0.908	2.600	2.762	5.140	5.351	0.232	0.190
186	4	5	3	2	2	2.580	2.792	4.780	5.544	0.155	0.304	1.590	2.088	3.320	3.982	− 0.131	0.021
187	4	5	3	4	2	2.760	3.042	5.520	6.165	0.309	0.431	1.710	2.101	3.480	4.045	− 0.107	0.032
188	4	5	3	6	2	3.060	3.293	6.300	6.787	0.469	0.558	1.800	2.113	3.620	4.108	− 0.079	0.042
189	4	5	3	8	2	3.400	3.543	6.960	7.408	0.603	0.685	1.880	2.126	3.730	4.173	− 0.053	0.053
190	4	5	3	10	2	3.610	3.793	7.610	8.029	0.727	0.812	1.930	2.138	3.790	4.239	− 0.042	0.064
191	4	5	3	2	3	2.400	2.640	4.410	5.066	0.090	0.207	1.360	1.617	3.050	3.154	− 0.196	− 0.106
192	4	5	3	4	3	2.720	2.890	5.020	5.687	0.213	0.334	1.370	1.626	2.850	3.204	− 0.234	− 0.095
193	4	5	3	6	3	3.050	3.140	5.750	6.309	0.355	0.461	1.410	1.636	2.880	3.254	− 0.221	− 0.084
194	4	5	3	8	3	3.340	3.390	6.460	6.930	0.496	0.588	1.480	1.646	3.040	3.305	− 0.192	− 0.074
195	4	5	3	10	3	3.580	3.641	7.090	7.551	0.633	0.715	1.610	1.656	3.290	3.357	− 0.141	− 0.063
196	4	5	3	2	4	2.350	2.487	4.200	4.588	0.045	0.111	1.230	1.252	2.770	2.499	− 0.250	− 0.233
197	4	5	3	4	4	2.690	2.737	4.750	5.209	0.157	0.238	1.250	1.259	2.640	2.538	− 0.270	− 0.222
198	4	5	3	6	4	3.030	2.988	5.360	5.831	0.272	0.365	1.310	1.267	2.640	2.578	− 0.268	− 0.211
199	4	5	3	8	4	3.230	3.238	6.080	6.452	0.419	0.492	1.340	1.274	2.680	2.618	− 0.262	− 0.200
200	4	5	3	10	4	3.550	3.488	6.690	7.073	0.546	0.619	1.450	1.282	2.920	2.659	− 0.212	− 0.190
201	4	5	3	2	5	2.330	2.335	4.120	4.110	0.023	0.015	1.130	0.969	2.560	1.979	− 0.292	− 0.359
202	4	5	3	4	5	2.630	2.585	4.520	4.731	0.108	0.142	1.140	0.975	2.400	2.010	− 0.317	− 0.349
203	4	5	3	6	5	2.980	2.835	5.130	5.353	0.231	0.269	1.180	0.981	2.400	2.042	− 0.321	− 0.338
204	4	5	3	8	5	3.180	3.085	5.780	5.974	0.364	0.396	1.260	0.987	2.510	2.074	− 0.294	− 0.327
205	4	5	3	10	5	3.530	3.336	6.400	6.596	0.483	0.523	1.350	0.993	2.700	2.107	− 0.255	− 0.316
206	4	5	3	2	6	2.260	2.182	4.020	3.632	0.005	− 0.081	1.050	0.751	2.390	1.568	− 0.322	− 0.486
207	4	5	3	4	6	2.580	2.432	4.360	4.253	0.075	0.046	1.050	0.755	2.240	1.592	− 0.346	− 0.475
208	4	5	3	6	6	2.840	2.683	4.910	4.875	0.186	0.173	1.100	0.759	2.280	1.617	− 0.350	− 0.464
209	4	5	3	8	6	3.120	2.933	5.540	5.496	0.313	0.300	1.150	0.764	2.360	1.643	− 0.328	− 0.454
210	4	5	3	10	6	3.520	3.183	6.160	6.118	0.442	0.427	1.270	0.769	2.510	1.669	− 0.296	− 0.443
						$R^2=0.781$		$R^2=0.892$		$R^2=0.827$		$R^2=0.803$		$R^2=0.824$		$R^2=0.782$	

E experimental results, *P* predicted results

References

Adler PM, Thovert JF, Mourzenko VV (2013) Fractured porous media. Oxford University Press, Oxford

Bahaaddini M (2017) Effect of boundary condition on the shear behaviour of rock joints in the direct shear test. Rock Mech Rock Eng 50(5):1141–1155

Barton N (1973) Review of a new shear-strength criterion for rock joints. Eng Geol 7(4):287–332

Belem T, Souley M, Homand F (2007) Modeling surface roughness degradation of rock joint wall during monotonic and cyclic shearing. Acta Geotech 2(4):227–248

Belem T, Souley M, Homand F (2009) Method for quantification of wear of sheared joint walls based on surface morphology. Rock Mech Rock Eng 42(6):883–910

Fathi A, Moradian Z, Rivard P, Ballivy G (2016) Shear mechanism of rock joints under pre-peak cyclic loading condition. Int J Rock Mech Min Sci 83:197–210

Fox DJ, Kana DD, Hsiung SM (1998) Influence of interface roughness on dynamic shear behavior in jointed rock. Int J Rock Mech Min Sci 35(7):923–940

Han G, Jing H, Jiang Y, Liu R, Su H, Wu J (2018a) The effect of joint dip angle on the mechanical behavior of infilled jointed rock masses under uniaxial and biaxial compressions. Processes 6(5):49

Han Z, Weatherley D, Puscasu R (2018b) Projected area-based strength estimation for jointed rock masses in triaxial compression. Comput Geotech 104:216–225

Heuze FE (1979) Dilatant effects of rock joints. In: Proc 4th ISRM congress, vol 1. Montreux, pp 169–175

Homand F, Belem T, Souley M (2001) Friction and degradation of rock joint surfaces under shear loads. Int J Numer Anal Meth Geomech 25(10):973–999

Hutson RW, Dowding CH (1990) Joint asperity degradation during cyclic shear. Int J Rock Mech Min Sci Geomech Abstr Pergam 27(2):109–119

Indraratna B, Haque A, Aziz N (1999) Shear behaviour of idealized infilled joints under constant normal stiffness. Géotechnique 49(3):331–355

Indraratna B, Welideniya HS, Brown ET (2005) A shear strength model for idealised infilled joints under constant normal stiffness. Geotechnique 55(3):215–226

Indraratna B, Thirukumaran S, Brown ET, Zhu SP (2015) Modelling the shear behaviour of rock joints with asperity damage under constant normal stiffness. Rock Mech Rock Eng 48(1):179–195

Jaeger JC (1971) Friction of rocks and stability of rock slopes. Geotechnique 21(2):97–134

Jafari MK, Pellet F, Boulon M, Hosseini KA (2004) Experimental study of mechanical behaviour of rock joints under cyclic loading. Rock Mech Rock Eng 37(1):3–23

Jiang Y, Tanabashi Y, Mizokami T (2001) Shear behavior of joints under constant normal stiffness conditions. In: Proc ISRM 2001-2nd ARMS, Beijing, pp 247–50

Jiang Y, Xiao J, Tanabashi Y, Mizokami T (2004) Development of an automated servo-controlled direct shear apparatus applying a constant normal stiffness condition. Int J Rock Mech Min Sci 41(2):275–286

Jiang Y, Li B, Tanabashi Y (2006) Estimating the relation between surface roughness and mechanical properties of rock joints. Int J Rock Mech Min Sci 43(6):837–846

Jing L, Stephansson O, Nordlund E (1993) Study of rock joints under cyclic loading conditions. Rock Mech Rock Eng 26(3):215–232

Johnston IW, Lam TSK, Williams AF (1987) Constant normal stiffness direct shear testing for socketed pile design in weak rock. Geotechnique 37(1):83–89

Kana DD, Fox DJ, Hsiung SM (1996) Interlock/friction model for dynamic shear response in natural jointed rock. Int J Rock Mech Min Sci Geomech Abstr Pergam 33(4):371–386

Lee HS, Park YJ, Cho TF, You KH (2001) Influence of asperity degradation on the mechanical behavior of rough rock joints under cyclic shear loading. Int J Rock Mech Min Sci 38(7):967–980

Li N, Chen W, Zhang P, Swoboda G (2001) The mechanical properties and a fatigue-damage model for jointed rock masses subjected to dynamic cyclical loading. Int J Rock Mech Min Sci 7(38):1071–1079

Li B, Jiang Y, Koyama T, Jing L (2008) Experimental study of the hydro-mechanical behavior of rock joints using a parallel-plate model containing contact areas and artificial fractures. Int J Rock Mech Min Sci 45(3):362–375

Li Y, Oh J, Mitra R, Hebblewhite B (2016) A constitutive model for a laboratory rock joint with multi-scale asperity degradation. Comput Geotech 72:143–151

Li Y, Wu W, Li B (2018) An analytical model for two-order asperity degradation of rock joints under constant normal stiffness conditions. Rock Mech Rock Eng 51(5):1431–1445

Liu R, Yu L, Jiang Y (2017a) Quantitative estimates of normalized transmissivity and the onset of nonlinear fluid flow through rough rock fractures. Rock Mech Rock Eng 50(4):1063–1071

Liu Y, Dai F, Fan P, Xu N, Dong L (2017b) Experimental investigation of the influence of joint geometric configurations on the mechanical properties of intermittent jointed rock models under cyclic uniaxial compression. Rock Mech Rock Eng 50(6):1453–1471

Liu Y, Dai F, Zhao T, Xu N (2017c) Numerical investigation of the dynamic properties of intermittent jointed rock models subjected to cyclic uniaxial compression. Rock Mech Rock Eng 50(1):89–112

Liu Y, Dai F, Dong L, Xu N, Feng P (2018) Experimental investigation on the fatigue mechanical properties of intermittently jointed rock models under cyclic uniaxial compression with different loading parameters. Rock Mech Rock Eng 51(1):47–68

Luo X, Jiang N, Wang M, Xu Y (2016) Response of leptynite subjected to repeated impact loading. Rock Mech Rock Eng 49(10):4137–4141

Mirzaghorbanali A, Nemcik J, Aziz N (2014) Effects of shear rate on cyclic loading shear behaviour of rock joints under constant normal stiffness conditions. Rock Mech Rock Eng 47(5):1931–1938

Oh J, Cording EJ, Moon T (2015) A joint shear model incorporating small-scale and large-scale irregularities. Int J Rock Mech Min Sci 76:78–87

Oh J, Li Y, Mitra R, Canbulat I (2017) A numerical study on dilation of a saw-toothed rock joint under direct shear. Rock Mech Rock Eng 50(4):913–925

Plesha ME (1987) Constitutive models for rock discontinuities with dilatancy and surface degradation. Int J Numer Anal Methods Geomech 11(4):345–362

Seidel JP, Haberfield CM (2002) A theoretical model for rock joints subjected to constant normal stiffness direct shear. Int J Rock Mech Min Sci 39(5):539–553

Shang J, West LJ, Hencher SR, Zhao Z (2018) Tensile strength of large-scale incipient rock joints: a laboratory investigation. Acta Geotech 13(4):869–886

Tse R, Cruden D (1979) Estimating joint roughness coefficients. Int J Rock Mech Min Sci Geomech Abstr 16(5):303–307

Wang G, Zhang X, Jiang Y, Wu X, Wang S (2016) Rate-dependent mechanical behavior of rough rock joints. Int J Rock Mech Min Sci 83:231–240

Wu B, Kanopoulos P, Luo X, Xia K (2014) An experimental method to quantify the impact fatigue behavior of rocks. Meas Sci Technol 25(7):075002

Wu J, Feng M, Yu B, Han G (2018a) The length of pre-existing fissures effects on the mechanical properties of cracked red sandstone and strength design in engineering. Ultrasonics 82(1):188–199
Wu X, Jiang Y, Li B (2018b) Influence of joint roughness on the shear behaviour of fully encapsulated rock bolt. Rock Mech Rock Eng 51(3):953–959
Yin Q, Ma G, Jing H, Wang H, Su H, Wang Y, Liu R (2017) Hydraulic properties of 3D rough-walled fractures during shearing: an experimental study. J Hydrol 555:169–184